Highway Safety and Traffic Flow Analysis of Mixed traffic with Connected and Non-Connected Vehicles

September 2022

A Research Report from the Pacific Southwest Region University Transportation Center

Petros Ioannou, University of Southern California

Fernando V. Monteiro, University of Southern California

TECHNICAL REPORT DOCUMENTATION PAGE

1. Report No. PSR-20-09	**2. Government Accession No.** N/A	**3. Recipient's Catalog No.** N/A
4. Title and Subtitle Highway Safety and Traffic Flow Analysis of Mixed traffic with Connected and Non-Connected Vehicles		**5. Report Date** September 3, 2022 **6. Performing Organization Code** N/A
7. Author(s) Petros Ioannou, USC https://orcid.org/0000-0001-6981-0704 Fernando V. Monteiro, USC https://orcid.org/my-orcid?orcid=0000-0002-6188-6971		**8. Performing Organization Report No.** PSR-20-09
9. Performing Organization Name and Address METRANS Transportation Center University of Southern California University Park Campus, RGL 216 Los Angeles, CA 90089-0626		**10. Work Unit No.** N/A **11. Contract or Grant No.** USDOT Grant 69A3551747109
12. Sponsoring Agency Name and Address U.S. Department of Transportation Office of the Assistant Secretary for Research and Technology 1200 New Jersey Avenue, SE, Washington, DC 20590		**13. Type of Report and Period Covered** Final report (Aug. 2020–Dec. 2021) **14. Sponsoring Agency Code** USDOT OST-R

15. Supplementary Notes
Report URL: https://www.metrans.org/research/highway-safety-and-traffic-flow-analysis-of-mixed-traffic-with-connected-and-non-connected-vehicles-

16. Abstract
Safety is the number one issue in the deployment of any vehicle technology. This leads to two interconnected challenges. First, how to ensure safety without having a significant negative impact in traffic flow. Second, how will varying penetrations of autonomous vehicles (AVs) impact safety and efficiency in mixed traffic. To address these issues, we start by proposing a risk metric that takes into account the severity of a collision that would happen under a worst-case scenario and the time the vehicle is exposed to such a collision. With this definition, we propose an autonomous lane changing procedure in which the vehicle behaves as if it was simultaneously on both lanes. This ensure that the vehicle never puts itself in a collision prone situation. Given the conservative nature of this approach, which can negatively impact traffic flow, we include the possibility of the AV accepting risks in its gap acceptance decision process. We extend this approach to a scenario with connected and autonomous vehicles (CAV), which can cooperate to generate lane change gaps through communications. In this case, a CAV in the destination lane also behaves as if it was simultaneously on two lanes, thus generating the gap for the incoming vehicle. We perform extensive micro simulations using the commercial software VISSIM with varying percentages of AVs and CAVs, different vehicle inputs, and several accepted risk values. Results indicate that, while AVs need to accept small risks in order to achieve the same traffic flow efficiency as humans, CAVs can improve both safety and efficiency without having to accept any risks. Our results also indicate that AVs and CAVs still behave safely in mixed fleets, but they do not bring significant improvements in traffic flow.

17. Key Words Autonomous vehicles; Connected vehicles; Lane changing; Merging control; Safety; Safety analysis; Traffic flow; Traffic flow rate	**18. Distribution Statement** No restrictions.		
19. Security Classif. (of this report) Unclassified	**20. Security Classif. (of this page)** Unclassified	**21. No. of Pages** 48	**22. Price** N/A

Form DOT F 1700.7 (8-72) Reproduction of completed page authorized

Pacific Southwest Region UTC
University Transportation Center

Contents

About the Pacific Southwest Region University Transportation Center

The Pacific Southwest Region University Transportation Center (UTC) is the Region 9 University Transportation Center funded under the US Department of Transportation's University Transportation Centers Program. Established in 2016, the Pacific Southwest Region UTC (PSR) is led by the University of Southern California and includes seven partners: Long Beach State University; University of California, Davis; University of California, Irvine; University of California, Los Angeles; University of Hawaii; Northern Arizona University; Pima Community College.

The Pacific Southwest Region UTC conducts an integrated, multidisciplinary program of research, education and technology transfer aimed at *improving the mobility of people and goods throughout the region.* Our program is organized around four themes: 1) technology to address transportation problems and improve mobility; 2) improving mobility for vulnerable populations; 3) Improving resilience and protecting the environment; and 4) managing mobility in high growth areas.

U.S. Department of Transportation (USDOT) Disclaimer

The contents of this report reflect the views of the authors, who are responsible for the facts and the accuracy of the information presented herein. This document is disseminated in the interest of information exchange. The report is funded, partially or entirely, by a grant from the U.S. Department of Transportation's University Transportation Centers Program. However, the U.S. Government assumes no liability for the contents or use thereof.

California Department of Transportation (CALTRANS) Disclaimer

The contents of this report reflect the views of the authors, who are responsible for the facts and the accuracy of the information presented herein. This document is disseminated under the sponsorship of the United States Department of Transportation's University Transportation Centers program, in the interest of information exchange. The U.S. Government and the State of California assumes no liability for the contents or use thereof. Nor does the content necessarily reflect the official views or policies of the U.S. Government and the State of California. This report does not constitute a standard, specification, or regulation. This report does not constitute an endorsement by the California Department of Transportation (Caltrans) of any product described herein.

Disclosure

Principal Investigator, Co-Principal Investigators, others, conducted this research titled, "Highway Safety and Traffic Flow Analysis of Mixed traffic with Connected and Non-Connected Vehicles" at Ming Hsieh Department of Electrical Engineering, Viterbi School of Engineering, University of Southern California. The research took place from 08/16/2020 to 08/31/2021 and was funded by a grant from the California Department of Transportation in the amount of $100,000. The research was conducted as part of the Pacific Southwest Region University Transportation Center research program.

Abstract

Safety is the number one issue in the deployment of any vehicle technology. This leads to two interconnected challenges. First, how to ensure safety without having a significant negative impact in traffic flow. Second, how will varying penetrations of autonomous vehicles (AVs) impact safety and efficiency in mixed traffic. To address these issues, we start by proposing a risk metric that takes into account the severity of a collision that would happen under a worst-case scenario and the time the vehicle is exposed to such a collision. With this definition, we propose an autonomous lane changing procedure in which the vehicle behaves as if it was simultaneously on both lanes. This ensure that the vehicle never puts itself in a collision prone situation. Given the conservative nature of this approach, which can negatively impact traffic flow, we include the possibility of the AV accepting risks in its gap acceptance decision process. We extend this approach to a scenario with connected and autonomous vehicles (CAV), which can cooperate to generate lane change gaps through communications. In this case, a CAV in the destination lane also behaves as if it was simultaneously on two lanes, thus generating the gap for the incoming vehicle. We perform extensive micro simulations using the commercial software VISSIM with varying percentages of AVs and CAVs, different vehicle inputs, and several accepted risk values. Results indicate that, while AVs need to accept small risks in order to achieve the same traffic flow efficiency as humans, CAVs can improve both safety and efficiency without having to accept any risks. Our results indicate that AVs and CAVs still behave safely in mixed fleets, but they do not bring significant improvements in traffic flow.

Highway Safety and Traffic Flow Analysis of Mixed traffic with Connected and Non-Connected Vehicles

Executive Summary

This project addresses the important topic of safety along an evolutionary deployment path where vehicles will eventually become autonomous and connected with each other and infrastructure. Along this path vehicles with different levels of automation and connectivity will have to co-exist and safety needs to be well understood and impact of safety measures on traffic flow need to be analyzed. In today's driving environment drivers perform vehicle maneuvers competing for space and time in order to improve their travel time. This practice often puts them in a risky situation for a short period of time. During that short time period a neighboring vehicle maneuver or lack of it may lead into collision. Autonomous vehicles (AVs) cannot be designed to take such obvious risks due to liability issues. This is particularly challenging when performing lane changes and merging in dense traffic environments. One important question is how to find a space to merge into without placing any vehicle in a collision prone situation. And, moreover, what is the traffic flow impact of doing so? To tackle this issue, we start by adopting a safety definition based on a worst-case braking scenario. We then define risk based on how much the vehicle violates the safe gap and for long it does so. Next, we propose a decentralized controller-agnostic approach for lane changes that guarantees safety. Moreover, we include the possibility to accept some level of risk in our lane changing approach so we can study how risk-taking impacts traffic flow. In our method, the merging vehicle operates as having two possible leaders, one in its own lane and one in the destination lane till the lane change maneuver is completed. We then consider connected and autonomous vehicles (CAVs), which can cooperate with each other to generate lane changing gaps. After the merging vehicle requests the creation of a safe gap in the destination lane, the future following vehicle in the destination lane cooperates by acting as if the merging vehicle has already changed lanes. We evaluate our approach through extensive simulations in VISSIM. We vary the number of vehicles entering the network, the types of vehicle in the network (human, autonomous or connected and autonomous), the percentages of each type of vehicle, and the accepted risks. We conclude that AVs which behave conservatively can have a negative impact in traffic flow of a highway. They can present similar flow as humans once they start accepting small lane changing risks. CAVs, thanks to cooperation, can be safe and efficient without having to accept any risks. The biggest challenge is in mixed traffic. Our simulations indicate that the AVs and CAVs still behave as expected around human driven vehicles. However, they only have significant positive impact on the general highway safety at high penetrations.

Introduction

The first priority of Autonomous Vehicles (AVs) is to improve safety in traffic [1]. However, the conservative AV behavior required to ensure safety may be detrimental for traffic flow. This safety/traffic flow trade-off is not always evident in scenarios that consider only longitudinal vehicle movement [2]. The challenge of ensuring safety without having a negative impact on traffic flow only becomes apparent when AVs need to perform lane change and merging maneuvers. This fact is corroborated by the literature on lane changing and merging algorithms that explicitly take into account the maneuver's impact on traffic, such as [3], [4], [5]. Therefore, we must focus on lane changes if our goal is to obtain safe and efficient AVs.

Lane changing is one of the most challenging maneuvers performed in traffic. It requires that the driver pay attention to several surrounding vehicles while adjusting the vehicle's longitudinal and lateral velocities. It is especially difficult to perform safe lane changes in congested environments, where multiple vehicles might be competing for the same space and relative velocities between lanes may be high. Therefore, it is not surprising that, while autonomous longitudinal control technologies, such as Adaptive Cruise Control (ACC) and emergency braking are already mature, autonomous lane changing is still an open challenge. So far, most of the research has focused on topics such as trajectory planning, lateral control and identification of acceptable lane change gaps. All of these subjects are necessary towards the goal of creating vehicles capable of performing autonomous lane changes. However, they alone do solve the issue of maneuvering in vehicle-dense environments. Humans deal with this difficult situation by sometimes putting themselves at risk for short periods of time. One approach for autonomous vehicles is to use information from the current traffic scenario to estimate surrounding drivers' intentions and make a decision based on the computed probabilities of collision [6]. Such methods tend to be computationally expensive and require either assumptions on "common" human behavior or on lots of data. Alternatively, one can opt for being conservative, and assuming some predefined worst-case scenario might happen at any time. This yields more assuredly safe behavior. The downside is a vehicle that might block traffic when trying to change into a lane with fast heavy traffic flow. Both approaches can benefit from vehicle connectivity. If communications from vehicle to vehicle (V2V) or from vehicle to infrastructure (V2I) is possible, autonomous vehicles no longer have to rely only on their sensors to make decisions. Moreover, once communication is established, cooperation becomes possible. Therefore, connectivity allows one to envision a system where safety is greatly improved without compromising traffic flow. In either connected or non-connected case, most published papers either measure the safety of a single maneuver or study the effect of a certain policy on traffic flow. As pointed out by the survey in [7], very few studies analyze the trade-off between safety and traffic flow.

To close this gap, we propose two risk-aware vehicle controllers, one non-connected and one connected. Both are based on a worst-case scenario assumption, and they have a parameter which allows them to take measurable risks. The main difference is that the connected controller can request cooperation from vehicles at the destination lane. We run extensive

simulations in the microssimulator VISSIM to compare safety and traffic flow of different levels of penetrations of these technologies and of different risk acceptance levels.

The rest of this report is organized as follows. Section 2 contains a literature review. Next, in section 3 we review the most commonly used risk assessment criteria for measuring safety, and we propose our own metric. Then, sections 4 and 5 present the non-connected and connected controllers respectively. The simulation framework, the main results and their analysis are shown in section 6. Finally, section 7 summarizes the main findings.

Literature Review

In this section, we analyze first the relevant literature in risk assessment and then the works which deal with safety and efficiency analysis of autonomous vehicles (AVs) and connected autonomous vehicles (CAVs). Whenever necessary, we highlight the differences of an existing work to ours.

Risk Assessment

Autonomous vehicles must avoid collisions. To do so, they must be able to identify situations that might lead to a collision. Therefore, the safety analysis of vehicle maneuvers starts by defining how to assess risk. [6] divides risk assessment techniques in growing complexity as: physics based, maneuver-based and interaction-aware. The increased complexity allows less conservative behaviors at the cost of higher computation times. In practice, the vehicle controller's need for real-time risk assessment along with the goal of estimating safety in a simulation scenario with thousands of vehicles make physics-based methods the best choice for our work. Thus, this review does not address maneuver-based or interaction aware methods. Risk assessment methods in the transportation field are commonly referred to as Surrogate Safety Measures (SSMs), given their capability of predicting situations with high risk of collision. In what follows we first present the most used SSMs. This review is mostly based on the surveys [8] and [9].

One of the simplest, oldest. and most adopted SSMs is Time-To-Collision (TTC) [10]. It measures the time it will take for two vehicles to collide in case they maintain their current speeds. Mathematically:

$$\mathrm{TTC} = \begin{cases} \dfrac{d}{v_i - v_{i-1}}, & \text{if } v_i > v_{i-1} \\ \infty, & \text{otherwise} \end{cases}$$

where d is the distance between two vehicles, v_i is vehicle i's speed, and vehicle $i-1$ is ahead of vehicle i. Many studies (see [9], table 2 for examples) focus on determining desirable or minimum safe TTC. Others have proposed extensions to TTC, such as the Modified TTC which considers constant accelerations [11]. Time Exposed Time-to-Collision (TET) and Time Integrated Time-to-Collision (TIT) were proposed by [12]. TET is defined as total time TTC is below safe threshold value, while TIT is integral of the TTC profile when TTC is below the safe

threshold value. All the TTC-based metrics suffer from the same issue [13,14]: they can only capture dangerous situations when vi−vi−1 is positive (or when current accelerations lead to positive relative velocity in the case of MTTC). To exemplify why this is an issue, picture the situation where one vehicle is following another at high speed, small inter-vehicle distance, and close to zero negative relative velocity. In this case, the TTC indicates no risk. However, a small velocity variation from either vehicle could quickly lead to a very low TTC. This fast variation would leave the following vehicle with little time to respond to a high-risk scenario.

Another simple time-based SSM is time headway. It describes the elapsed time between the moment a leading vehicle passes a point on the road and the moment the following vehicle passes the same point. Mathematically:

$$H = t_\ell - t_f$$

where t_ℓ and t_f denote the time at which the leading and following vehicles, respectively, pass a certain fixed location on the road. Time headway has been extensively used to evaluate the safety of human car following behavior, with the recommended value in seconds varying from country to country [15]. The matter of defining desired time headway for autonomous vehicles has also been discussed in the literature. In [16], the minimum time headway to guarantee spacing error attenuation on a string of vehicles with first-order actuator dynamics was found. This result was extended to CAVs with faulty communications by [17]. While these findings are important in the design of longitudinal controllers, they do not provide any safety guarantees in terms of collision avoidance. The approach from [18] presented a method and assumptions to derive a collision-free headway based on a worst-case braking scenario.

The most commonly used deceleration based SSM is the Deceleration Rate to Avoid Crash (DRAC) [19]:

$$\text{DRAC} = \begin{cases} \dfrac{(v_i - v_{i-1})^2}{2d}, & \text{if } v_i > v_{i-1} \\ 0, & \text{otherwise} \end{cases}$$

where $d(t)$ is the distance between two vehicles, v_i is vehicle i's speed, and vehicle $i-1$ is ahead of vehicle i. Other deceleration based SSMs are the deceleration to bring relative speed to zero, and the Criticality Index Function (CIF) [20]. The Crash Potential Index is the probability that DRAC exceeds the vehicle's maximum available deceleration rate (MADR) [21]:

$$\text{CPI} = \frac{\sum_{t=0}^{N} P\,(DRAC(t) > MADR)\Delta t}{T}$$

where $P(A)$ is probability of event A, N is the total number of intervals, Δt is observation time interval, and T is total observation time ($T = N\Delta t$). MADR is often modeled as a truncated normal distribution. All these metrics suffer from the same issue as TTC, because they are also only defined for scenarios where vehicles are in collision route.

Some works focused on AVs proposed their own risk assessment techniques, which are then used to guide decision making, trajectory planning or vehicle control methods. In [22], the vehicle following risk was defined as the safe gap divided by the current gap. The authors then expanded the same concept to define lateral risks. This definition, as well as most of the SSMs described before, does not differentiate between severe or light collisions. The work in [23] addressed collision severity by defining the risk between two vehicles as the sum of their individual kinetic energies and of a "cross term" which depends on their relative velocity. A similar concept is used in [24] where the severity of a collision was defined as an exponential function of the ego vehicle's kinetic energy. These definitions of severity follow from the intuitive notion that kinetic energy is related to collision severity. Nonetheless, the literature of accident analysis has long established that the main predictor of injury in a crash is the magnitude of the velocity change experienced by a vehicle during the crash [25–27]. This metric is known as Delta-V. Details on how to compute Delta-V can be found in [28]. Both [14] and [13] argue for incorporating Delta-V to risk assessment techniques. In section 3, we expand the approach from [18] to compute headway values that yield, in the worst-case scenario, a collision with bounded Delta-V. This risk metric can be easily integrated in lane changing gap acceptance methods.

Longitudinal Adjustments and Gap Acceptance for Lane Changing and Merging

We start by reviewing works on gap acceptance and longitudinal adjustments which implicitly define safety as the lack of collisions. Then we present previous works that used risk assessment techniques to view safety in a non-binary way.

With a focus on determining lane change safety, the work in [29] used a sinusoidal lateral acceleration model alongside constant speed assumptions to compute longitudinal safe gaps between an ego vehicle and the surrounding vehicles before starting the lane change. Then, in [30], the possibility of emergency braking during the lateral movement is taken into account when determining safe distances. These results were used in [31] to analyze safety of platoon maneuvers. More recently, works [32] and [33] applied the results from [29] to propose safe multi-vehicle lane change planning. By including the possibility of lateral evasive maneuvers, less conservative safe gaps were computed in [34]. A different approach was taken in [35], where, instead of measuring and checking for safe gaps, vehicles consider a maneuver to be safe based on the deceleration they will force on their future follower. Still dealing with maneuver feasibility, perception uncertainty was explicitly included in [36] and [37].

Building on these results, other studies addressed the issue of generating the necessary gaps when these do not exist. To guarantee maneuver safety and feasibility in busy traffic scenarios, numerous solutions rely on Connected Autonomous Vehicles (CAVs). These vehicles can communicate either with other vehicles (V2V) or with the infrastructure (V2I) through standards such as Dedicated Short-Range Communications (DSRC) [38]. After establishing a connection, they can cooperate with each other to overcome the previously described difficulties. This idea was already applied in cooperative merging [4], where highway vehicles make space for on-ramp incomers. Despite the success of these methods, they cannot be

directly applied to the more general case of lane changes. The fact that merging must occur within a predefined area often yields procedures that depend on the existence of a roadside unit which can communicate to vehicles, perform a centralized optimization, and determine the merging order [39]. The main idea we borrow from this domain, as will be seen later, is the one of virtual vehicles [40].

In [41], a vehicle in the destination lane uses a Linear Quadratic Regulator (LQR) to increase the distance to its leader and generate the necessary gap for the lane changing vehicle. Both [42] and [43] create the safe gaps by changing the setpoint of the constant time headway controller already in place. Instead of collaboration, the authors of [44] propose that vehicles negotiate based on their cost functions to decide whether to accelerate or decelerate before a lane change. However, none of these approaches discussed how to keep the lane changing vehicle at the proper position to initiate the maneuver, which means they are not suited for congested scenarios. The work in [45] adopted a nonlinear longitudinal controller derived from artificial potential fields, but it makes simplifying assumptions that do not hold in congested environments. In the approach of [46], the lane changing vehicle and of the vehicle generating gap have access to each other's MPCs in order to minimize the maneuver's impact on traffic.

Defining safety as the lack of accidents is intuitive, but it is not practical for the study of the macroscopic effects of autonomous vehicles in traffic. First, as noted by the survey in [47], accidents are rare events, which means both simulations and real-life tests would have to run for enormous amounts of time to provide an estimate of the number of crashes produced or avoided by a new technology. Second, in vehicle dense environments, the AV must be able to differentiate between more or less risky actions to be able to avoid collision-prone situations. Risk can be included in cost functions when lane changing decisions are formulated as optimization [22,48] or game theory [49–52] problems. Safety was assessed based on violation of a safety distance [22, 51, 52], time headway [50], or a combination of approaching speed and distance [48, 49]. In all these cases, the goal was to minimize the final risk, but we cannot determine beforehand what is the maximum risk accepted by a vehicle. It is therefore not possible to evaluate how risk acceptance would impact these methods. The approach from [53] defined risk as the probability of collision, and the AV decided which maneuver to take based on an accepted risk value. It is not clear if the approach can be extended lane changing in congested scenarios, where vehicles must continuously adjust their speeds and check for available lane change gaps. Moreover, none of the works mentioned here studied how their methods would impact traffic on a macroscopic scale.

Safety/Efficiency Trade-Off of AVs and CAVs

Once a method to deal with congested scenarios is shown to create safe behavior, we must also evaluate its impact on traffic flow. Numerous works have used risk assessment techniques along with AV and CAV models to study the impact of such technologies on traffic. A recent review of the topic can be found in [54]. The effects on safety and flow of longitudinally automated vehicles have been studied on roundabouts by [55], T-junctions by [56], intersections by [57] and highways by [58] and [59]. Each of these studies presented its own longitudinal controller, but they did not include methods specific to automated lane changes. In

[2], the effects of autonomous vehicles with and without communications on traffic flow were analyzed in depth, but safety was not evaluated and cooperative lane changing is not considered. The work from [60] analyzed the influence of longitudinal behavior, lane change intention and gap acceptance of vehicles with no automation, partial automation, and conditional automation (as defined by SAE International) on traffic flow. However, the authors did not use a verified traffic simulator and there was no safety analysis. Using the simulator PELOPS, [61] evaluated how safety measurements varied under different market penetrations of automated vehicles, but traffic flow results were not presented. Furthermore, the proposed automated vehicles did not operate in high vehicle density scenarios. [62] used the traffic simulator VISSIM along with the Surrogate Safety Assessment Model (SSAM) software, described in [63], to inspect the impacts of platoon forming CAVs on a highway. Results showed that CAVs reduced the number of conflicts considerably at the cost of an increased travel times.

VISSIM is also used in [64] to investigate how lane change recommendation signs together with cooperative lane changing can improve throughput on a highway with one closed lane. Safety evaluation is restricted to the analysis of acceleration and speed variations. The VISSIM scenario in [65] and [66] includes highways, signalized intersections, and priority junctions. Together, these two papers studied safety, as measured by the number of conflicts in SSAM, and traffic flow impacts of increasing market penetration of CAVs with cooperative lane changing capabilities. They concluded, in contrast with [62], that CAVs improved total system travel time, at the cost of more conflicts between human-driven vehicles and CAVs. Both [62,65] used the SSAM [63] to evaluate safety. However, SSAM defines a conflict as “a scenario where two road users will likely collide without evasive action”. Our proposed risk metric, on the other hand, has positive values whenever a vehicle is in a position that could lead to a collision if the worst-case scenario happens. Moreover, [65] mentions that SSAM is not suitable to analyze safety between interacting AVs. Last, none of these works analyzed how risk-acceptance would impact traffic flow.

Risk Assessment Criteria

As noted in [67], each risk assessment technique has its advantages and shortcomings. Given that AVs are expected to actively avoid collision-prone situations, we need a metric that not only identifies imminent collision risk, but that also ensures that the vehicle has enough time and space to avoid collisions in a worst-case scenario. Moreover, since we intend to study how risk-taking affects traffic, the metric must have continuous values. To fulfill these requirements, we propose the following.

Definition 1. The risk at any time t equals the severity of a collision that would occur at some time $t_c > t$ in case a predefined worst-case braking scenario occurs. If there would be no collision under the worst-case braking scenario, then the risk is zero.

In the remainder of this section, we define a worst-case braking scenario and present the resulting safe gap. We then apply the definition of Delta-V to compute the severity of collisions that might happen in case the safe gap is not respected. We focus on vehicle following for most

of the section and present the modifications needed to extend the approach to lane changing at the end.

Worst-case Braking Scenario and Safe Gap

Let the ego vehicle E be following a leading vehicle ℓ as illustrated by Figure 1.

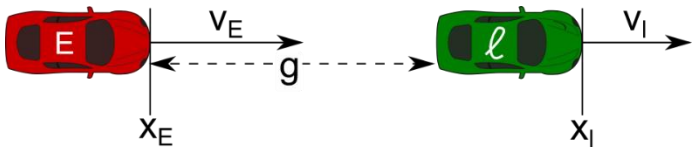

Figure 1 Illustration of a vehicle following scenario.

The gap between the vehicles is:

$$g(t) = x_\ell(t) - l_\ell - x_E(t)$$

where x_E, x_ℓ are the ego and leading vehicles, respectively, front-bumper positions, and l_ℓ is the leading vehicle's length. Following from the risk definition, a safe vehicle following gap is the distance between two vehicles that allows the ego vehicle to achieve full stop under a worst-case braking scenario. We define the worst-case braking scenario as in Figure 2. It represents the situation where the leading vehicle, ℓ, undergoes emergency braking and how the ego vehicle, E, responds. It represents the situation where the leading vehicle, ℓ, undergoes emergency braking and how the ego vehicle, E, responds. At t_0, the leader applies maximum deceleration d_ℓ, and it keeps this deceleration until full stop, which happens at t_ℓ. At t_0, the following vehicle might have some positive acceleration $\bar{a}_E$. After a time interval τ_d, that includes perception, communication (in the case of connected vehicles) and computation delays, the following vehicle is aware that its preceding vehicle has started an emergency braking maneuver. It responds by applying maximum braking, characterized by a maximum jerk j_E and a maximum deceleration d_E. The negative jerk phase lasts for a time interval τ_j. We assume that the initial inter-vehicle gap is big enough so that the vehicles do not collide before the following vehicle achieves its maximum deceleration. Last, the following vehicle decelerates at d_E until it achieves full-stop at time t_E. The interval τ_d is used to differentiate between human, autonomous and connected followers. Human drivers present the highest delays. Both autonomous and connected vehicles have considerably faster reaction times than humans. While autonomous vehicles have to rely only on their own sensors to identify if the leader is performing an emergency braking maneuver, connected vehicles can know about it after a single communication delay. Therefore, connected vehicles achieve the lowest values of τ_d.

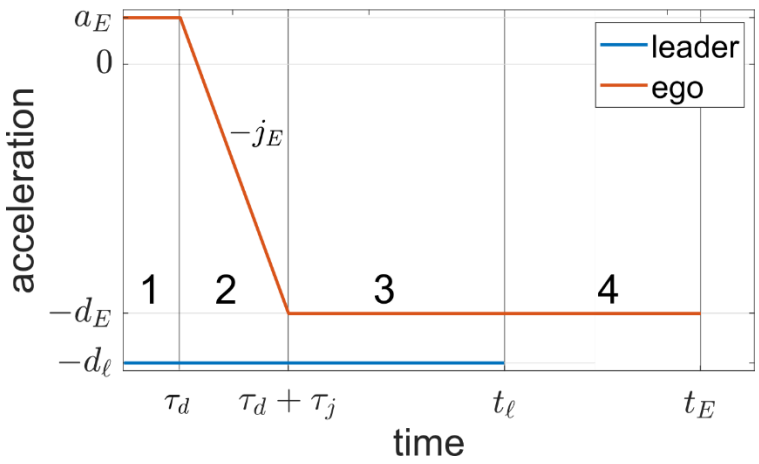

Figure 2 Worst-case braking scenario acceleration profiles. The numbers identify each of the relevant time intervals.

The vehicle following gap changes over time following:

$$\begin{aligned} g(t) &= g_0 + \Delta g(t_0, t) \\ \Delta g(t_0, t) &= \big(v_\ell(t_0) - v_E(t_0)\big)(t - t_0) + \int_{t_0}^{t}\int_{t_0}^{\lambda} \big(a_\ell(\tau) - a_E(\tau)\big)\,(\tau)\mathrm{d}\tau\lambda \end{aligned} \quad (1)$$

where t_0 is the initial time, $g_0 = g(t_0)$, $v_\ell(t_0)$, $v_E(t_0)$ are the initial speeds of vehicles ℓ and E, respectively, and $a_\ell(t)$, $a_E(t)$ are their respective accelerations. The gap $g(t_0)$ is considered safe if $g(t_E) > 0$, where t_E is the time the ego vehicle achieves full stop. Therefore, we need to solve:

$$\begin{aligned} g_0 &> -\Delta g(t_0, t), \quad t \in [t_0, t_E] \\ g_0 &> \max_{t\in[t_0,t_E]} -\Delta g(t_0, t) \end{aligned}$$

Solving for the worst-case scenario, we get:

$$g_0^* = \begin{cases} \dfrac{(v_E(t_0) + \lambda_1)^2}{2d_E} - \dfrac{v_\ell^2(t_0)}{2d_\ell} + \lambda_0, & \text{if } t_E \geq t_\ell, \\ \dfrac{(v_\ell(t_0) - v_E(t_0) - \lambda_1)^2}{2(d_E - d_\ell)} + \lambda_0, & \text{if } t_E < t_\ell \text{ and } d_\ell < d_E \\ 0, & \text{otherwise} \end{cases} \quad (2)$$

where

$$\lambda_0 = -\frac{\bar{a}_E + d_E}{2}\left(\tau_d^2 + \tau_d\tau_j + \frac{\tau_j^2}{3}\right) \quad (3)$$

$$\lambda_1 = (\bar{a}_E + d_E)\left(\tau_d + \frac{\tau_j}{2}\right), \quad (4)$$

and $\tau_j = (\bar{a}_E + d_E)/j_E$. We note that the condition $t_E \geq t_\ell$ can be expressed in terms of the initial conditions and relative braking capability:

$$\frac{v_E(t_0) + \lambda_1}{d_E} \geq \frac{v_\ell(t_0)}{d_\ell}$$

In [18], we made use of the vehicle's free-flow speed and assumed a bound on $v_\ell(t_0) - v_E(t_0)$ to find a desired gap:

$$g_d(t_0) = h v_E(t_0) + c \geq g_0^* \quad \textbf{(5)}$$

such that $g_d(t_0) > g_0^*$ for any t_0. The value h is known as the time headway, and c is the desired distance at low speeds. The advantage of using linear safety constraints is twofold. First, they are less sensitive to noise in the measurement of $v_E(t)$, and they are independent of any noise in the measurement of $v_\ell(t)$. Second, these constraints are simple enough to be easily integrated in existing longitudinal controllers. Next, we can define the severity of a collision if the safe gap is not respected.

Severity of Collision

If the inter-vehicle gap between the ego vehicle E and its leader ℓ is such that there is a collision under the worst-case braking scenario, the collision severity can be estimated by a measure called Delta-V [13, 14, 25, 27, 28]. Delta-V is defined as the magnitude of the difference in the vehicle's velocity right before and right after the impact. If we assume a purely longitudinal perfectly inelastic collision, the sum of Delta-Vs for both vehicles is:

$$\text{Delta-V}(t_c) = v_E(t_c) - v_\ell(t_c) \quad \textbf{(6)}$$

where v_E, v_ℓ are the speeds of the ego and leading vehicles, and t_c is the collision time. The assumption of perfectly inelastic collision is common for longitudinal collisions [68,69]. We also note that a collision can only occur when $v_E(t_c) \geq v_\ell(t_c)$, thus Delta-V$(t_c)$ is always non-negative. Applying the worst-case scenario definition, we can find $v_E(t_c)$ and $v_\ell(t_c)$ based on the initial gap g_0 and on the velocities at the start of the braking scenario $v_E(t_0)$ and $v_\ell(t_0)$. From kinematics, we know that the ego vehicle's longitudinal speed at the collision time t_c is:

$$v_E(t_c) = \begin{cases} v_E(t_0) + \bar{a}_E t_c, & \text{if } t_c < \tau_d \\ v_E(t_0) + \bar{a}_E t_c - 1/2\, j_E (t_c - \tau_d)^2, & \text{if } \tau_d \leq t_c < \tau_d + \tau_j \\ v_E(t_0) + \bar{a}_E \left(\tau_d + \frac{\tau_j}{2}\right) - d_E \left(t_c - \tau_d - \frac{\tau_j}{2}\right), & \text{if } \tau_d + \tau_j \leq t_c < t_E \end{cases} \quad \textbf{(7)}$$

where $\bar{a}_E$, j_E and d_E are, respectively, the ego vehicle's longitudinal initial acceleration, maximum jerk, and maximum deceleration. Time intervals τ_d and τ_j represent the reaction delay and the negative jerk phase respectively, and t_E is the time it takes for vehicle E to achieve full stop. Following the same reasoning, the leader's speed at collision time is

$$v_\ell(t_c) = \begin{cases} 0, & \text{if } t_\ell < t_c \\ v_\ell(t_0) - d_\ell t_c, & \text{if } t_\ell \geq t_c \end{cases} \quad (8)$$

where d_ℓ is the leader's maximum deceleration and t_ℓ is the time it takes for vehicle ℓ to achieve full stop. The computation of t_c is detailed in the Appendix. An example of Delta-V versus initial gap for the worst-case braking scenario with parameters as in Table 1 is illustrated in Figure 3.

Table 1 Parameters of Delta-V Computation Example

$v_E(t_0)$	$v_\ell(t_0)$	τ_d	d_ℓ	$a_E(t_0)$
90 km/h	90 km/h	0.2 s	8 m/s^2	0.6 m/s^2

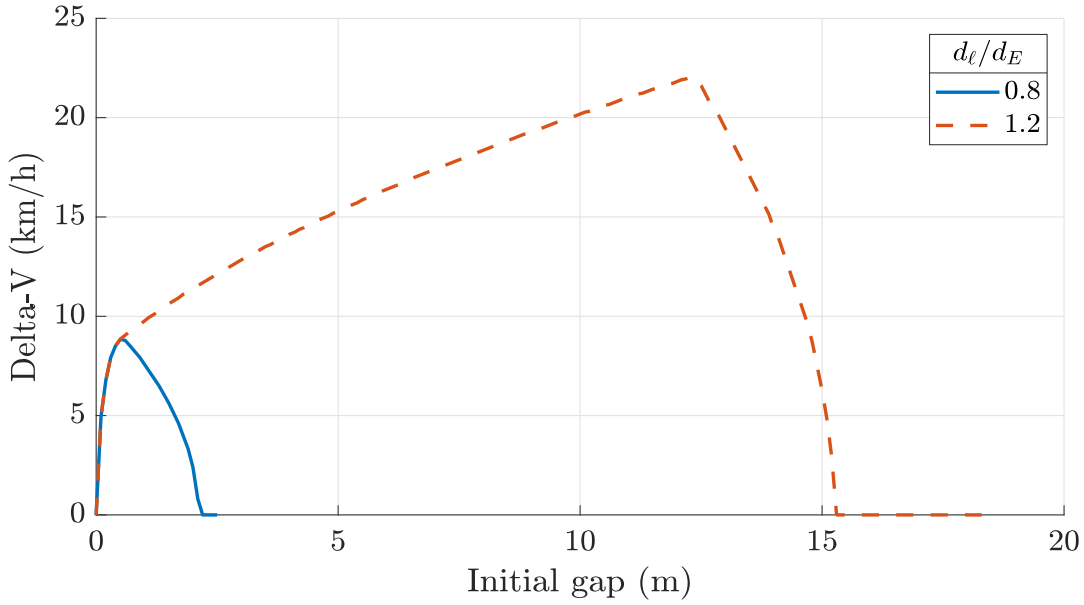

Figure 3 Delta-V as a function of the initial gap under the worst-case scenario

Now that the worst-case scenario and the severity metric have been clearly defined, Definition 1 leads to the following risk metric:

$$r(t_0) = \text{Delta-V}(t_c), \text{ assuming the worst-case braking scenario starts at } t_0$$

for any t_0.

As previously mentioned, we focus on risk taking during lane changes, since the safety/ efficiency trade-off is only seen when we include these maneuvers. Thus, we will now show how to expand the obtained results to lane changing and we will define the risk metric used in simulations.

Extension to Lane Changing and Merging

When a vehicle has the intention to perform a lane change, it must observe gaps to three surrounding vehicles: the leader in the origin lane ℓ_o, the leader in the destination lane ℓ_d, and to the follower in the destination lane f_d. The situation is illustrated in Figure 4. We assume that, if either of the leaders (at origin or destination lane) performs emergency braking during the ego vehicle's lane change, the ego vehicle responds like in the vehicle following case (as illustrated in Figure 2). Similarly, if the ego vehicle performs an emergency braking, the follower at the destination lane, f_d, also responds as in the vehicle following case. The main difference is that the ego vehicle has to consider the loss in braking capability during lateral movement. Therefore, the value of d_E in all the safe gap and risk computations between E and either ℓ_o or ℓ_d has to be reduced. Lateral evasive maneuvers that the ego vehicle could take to avoid collision are intentionally disregarded. We do this in order to keep the worst-case scenario simple and with few assumptions. The last factor to consider is the possible significant relative velocity between the ego vehicle and vehicles in the destination lane. Taking all these points into account, we conclude that a lane change starting at time t_0 is collision free with respect to the worst-case braking scenario of Figure 2 if the three gaps indicated in Figure 4 satisfy:

$$g(t_0) \geq g^*(t_0) + \Delta g(t_0, t_{\text{lc}})$$

where g_0^* is computed as in Eq.(2)(2), t_{lc} is the time when the lane change is completed, and $\Delta g(t_0, t_{\text{lc}})$ represents the inter-vehicle gap variation during the lane change maneuver assuming constant speeds. We can assume constant speeds during lane changing because the term $g^*(t_0)$ already takes the worst-case braking scenario into account. Moreover, the result from Eq. (5 **)** can be applied again leading to:

$$g(t_0) \geq hv_E(t_0) + c + \Delta g(t_0, t_{\text{lc}})$$

It is important to highlight that g_0^* and h between the ego vehicle and either of the leaders must be computed assuming a reduced value for the ego vehicle's maximum braking. During a lane change, we always compute the risk between E and the three surrounding vehicles following Eqs. (6) to (8)

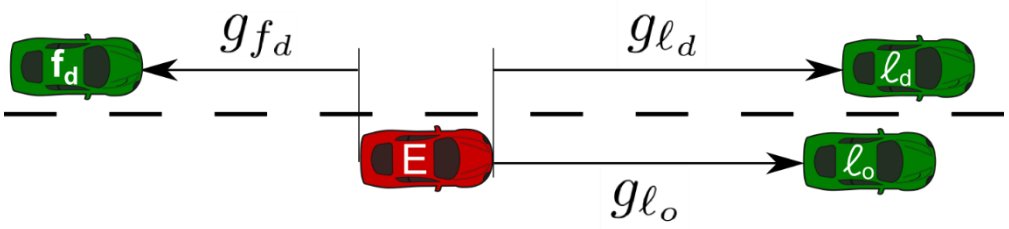

Figure 4 The ego vehicle must check three gaps before deciding whether a lane change is safe.

To compare the risk taken by human driven vehicles, AVs and CAVs during lane changing, one must take the time a vehicle is exposed to collision into account. Assuming the lane change maneuver starts at t_0 and ends at t_{lc}, the total risk of each lane change is measured by:

$$R = \sum_{k=\{\ell_o, \ell_d, f_d\}} \int_{t_0}^{t_{lc}} r_k(\tau) \mathrm{d}\tau$$

where $r_k(t)$ denotes the risk between the lane change vehicle and one of its surrounding vehicles. Let there be N lane changes during a simulation, each one with a risk R_i, where $i = \{1, \dots N\}$. If $R_i > 0$, we call that a *risky lane change*. In section 6 we use the number of risk lane changes during a simulation as a risk assessment metric. Moreover, we compute the median value of R among the risky lane changes.

The equations presented so far can be used to evaluate the risks taken by a vehicle in a simulation setting, but they have some shortcomings in terms of applicability. First, we note that the Delta-V computation demands exact knowledge of the states and braking capabilities of both vehicles. Moreover, it depends nonlinearly on parameters which we cannot expect to know with great precision. Last, the example in Figure 3 shows that small gaps lead to the same Delta-V as gaps close to the safe gap value. This ignores the fact that collisions at high speeds may have harder to predict consequences than collisions with equal Delta-V at lower speeds. These issues make the theoretical computation of Delta-V unsuitable for any real-world application and for integration in commonly used longitudinal controllers. In the next section we present the necessary assumptions to obtain an upper bound on severity that is independent of the leader velocity and the current gap.

Risk Factors for Autonomous Vehicles

In this section we propose control algorithms for autonomous vehicles that receive risk as a parameter. We start by showing how risk acceptance impacts the desired time headway and the lane changing gaps. Then, we propose the risk-taking lane changing method. After that, we present the implementation of longitudinal controllers used in the simulations. We end the section with a note on how autonomous vehicles behave in mixed traffic.

Time Headway and Lane Changing Gaps with Risk

As noted in section 3, the computation of the theoretical value of Delta-V has some shortcomings which prevent it from being used outside simulation environments or in vehicle controllers. We want to be able to conservatively upper bound the severity with a formula that is independent of the leader velocity and current gap. It is also desirable that the upper bound decreases with the initial time headway. To obtain that, we follow an approach similar to [18]. First, let there be a free-flow speed $V_f \geq v_E(t)$, $\forall t$. Next, let $(1-\rho)v_E(t_0) \leq v_\ell(t_0) \leq v_E(t_0)$, where $0 \leq \rho \leq 1$. The upper bound on $v_\ell(t0)$ is a conservative assumption. The lower bound is determined by parameter ρ, which describes the maximum proportional relative speed difference between vehicles. The value of ρ is a design parameter and should be related to how closely the vehicle following controller is able to track the leading vehicle's speed. After tedious algebra, we can overestimate Delta-V squared as:

$$\text{Delta-V}^2(t_c) \leq \begin{cases} (\rho^2 V_f + 2\rho\lambda_1)v_E(t_0) + \lambda_1^2 - 2d_E(1-\gamma)(g_0 - \lambda_0), & \text{if } \gamma < \Gamma \\ \left(\dfrac{\gamma - (1-\rho)^2}{\gamma} V_f + 2\lambda_1\right) v_E(t_0) + \lambda_1^2 - 2d_E(g_0 - \lambda_0), & \text{if } \gamma \geq \Gamma \end{cases}$$

where λ_0 and λ_1 are as in Eqs. (3) and (4), and:

$$\gamma = d_\ell / d_E$$
$$\Gamma = (1-\rho)\frac{V_f}{V_f + \lambda_1}$$

We note that the upper bound on Delta-V^2 is a linear function of the ego vehicle's velocity. (a) (b)

Figure 5 shows examples of the theoretical Delta-V and its upper bound. The parameters are as

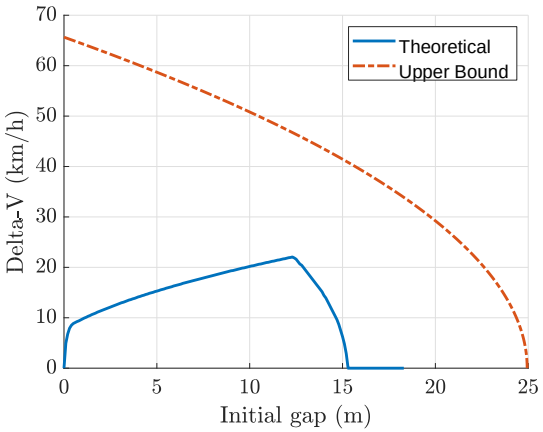

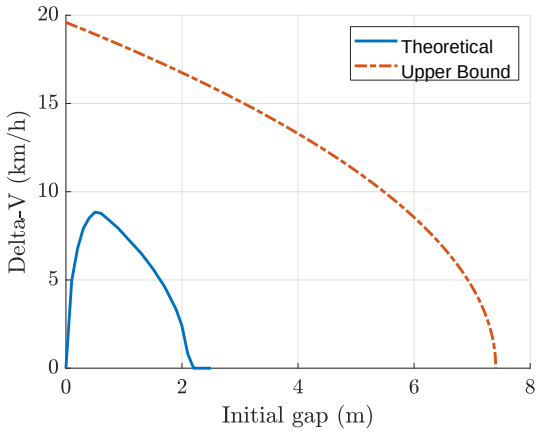

in Table 1 and $V_f = 108\,km/h$, $\rho = 0.1$.

(a) (b)

Figure 5 Theoretical Delta-V (solid blue) and its upper bound (dashed red) as a function of the initial gap under the worst-case scenario. In (a), the leader can brake harder than the ego vehicle: $d_E = d_\ell/1.2$. In (b), the ego vehicle can brake harder than the leader: $d_E = d_\ell/0.8$

Let r_a be the accepted risk. By setting r_a equal to the upper bound of Delta-V, we can obtain a reference gap $g_r(t)$:

$$g_r(t) = \begin{cases} \dfrac{1}{(1-\gamma)d_E}\left(\dfrac{\rho^2}{2}V_f + \rho\lambda_1 - \dfrac{r_a^2}{2V_f}\right)v_E(t_0) + \dfrac{\lambda_1^2}{2(1-\gamma)d_E} + \lambda_0, & \text{if } \gamma < \Gamma \\ \dfrac{1}{d_E}\left(\dfrac{\gamma - (1-\rho)^2}{2\gamma}V_f + \lambda_1 - \dfrac{r_a^2}{2V_f}\right)v_E(t_0) + \dfrac{\lambda_1^2}{2d_E} + \lambda_0, & \text{if } \gamma \geq \Gamma \end{cases}$$

This can be written as:

$$g_r(t) = h(r_a)v_E(t) + c$$

where $h(r_a)$ is the time headway measured in seconds. Setting:

$$h(r_a) = \begin{cases} \frac{1}{(1-\gamma)d_E}\left(\frac{\rho^2}{2}V_f + \rho\lambda_1 - \frac{r_a^2}{2V_f}\right), & \text{if } \gamma < \Gamma \\ \frac{1}{d_E}\left(\frac{\gamma-(1-\rho)^2}{2\gamma}V_f + \lambda_1 - \frac{r_a^2}{2V_f}\right), & \text{if } \gamma \geq \Gamma \text{ and } \gamma > (1-\rho)^2 \\ \frac{1}{d_E}\left(\lambda_1 - \frac{r_a^2}{2V_f}\right), & \text{if } \gamma \geq \Gamma \text{ and } \gamma \leq (1-\rho)^2 \end{cases}$$

$$c = \begin{cases} \frac{\lambda_1^2}{2(1-\gamma)d_E} + \lambda_0, & \text{if } \gamma < \Gamma \\ \frac{\lambda_1^2}{2d_E} + \lambda_0, & \text{if } \gamma \geq \Gamma \end{cases}$$

guarantees $r(t) \leq r_a, \forall t$. Following the same argument, lane change gaps which respect:

$$g(t_0) \geq h(r_a)v_E(t_0) + c + \Delta g(t_0, t_{lc}),$$

yield a lane change risk of at most r_a. It is important to highlight that $h(r_a)$ for lane changing between the ego vehicle and the two leaders must be computed assuming a reduced value for the ego vehicle's maximum braking.

Risk-Taking in Lane Changes

This section presents the control-agnostic lane changing method that guarantees bounded risk at all times. We focus on two aspects of the vehicle behavior: the longitudinal adjustment before starting a lane change and the gap acceptance decision. Under this framework, we view merging as a particular case of lane changing which must occur before a predefined position. The intention to make lane changes is assumed to come from a higher-level decision algorithm which chooses desired lanes based on perceived speed gains (for discretionary lane changes) or on routing requirements (for mandatory lane changes). Our proposed approach ensures that, if the worst-case braking scenario takes place by any vehicle involved, the collision severity is at most some accepted risk value r_a. We assume that an AV:

- reliably measures its own velocity and acceleration as well as the relative velocity between itself and the surrounding vehicles illustrated in Figure 4;
- can conservatively estimate the maximum acceleration of vehicles in its vicinity thanks to computer vision algorithms and databases. For example, the AV should be able to differentiate a truck from a passenger vehicle.

The AV does not have any knowledge about surrounding vehicles' accelerations. Since the gap acceptance algorithm ensures that vehicles only perform lane changes when safety constraints are respected, the challenge of designing trajectories is greatly simplified and existing approaches, such as the ones described in [71,72], can be used.

The AV's lane changing, and longitudinal adjustment decision process is summarized by the flowchart of Figure 6. Once the ego vehicle E has lane change intention, it sets an accepted risk

value r_a. After setting the risk, the vehicle checks whether the three surrounding gaps shown in Figure 4 yield a risk of at most r_a, i.e., whether they satisfy inequality (27). It is important to highlight three points at this step. First, E can set $r_a = 0$, which means only collision-free gaps will be accepted. Second, E could choose different values of r_a for each surrounding vehicle. Last, E must take into account its reduced braking capability to estimate the safe gaps, and that it estimates the safe gaps using conservative assumptions on other vehicle's braking capabilities. If the gaps accepted, the lane change maneuver can be completed. If not, we check whether there is a leader in the destination lane (ℓ_d). Let us first assume ℓ_d exists. In this case, the vehicle must decide whether to overtake or to merge behind the destination lane leader.

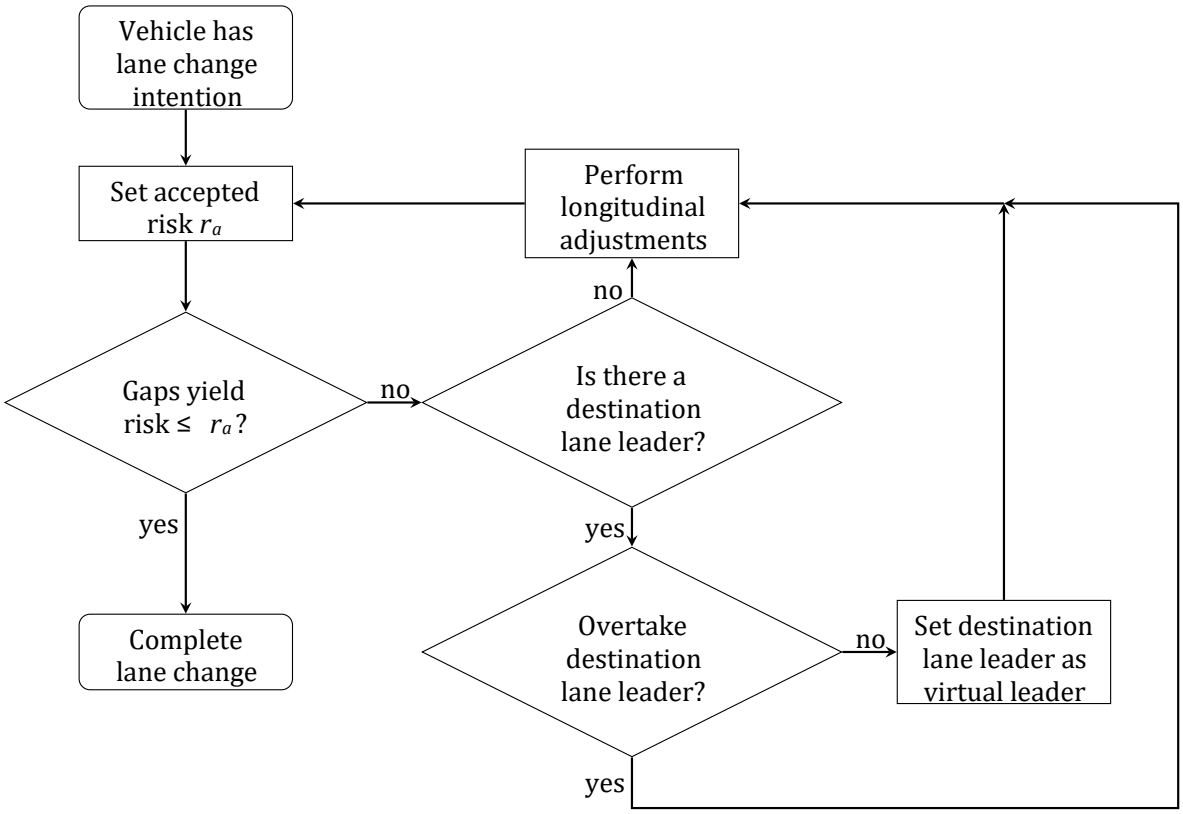

Figure 6 Autonomous vehicle flowchart for longitudinal adjustment and gap acceptance.

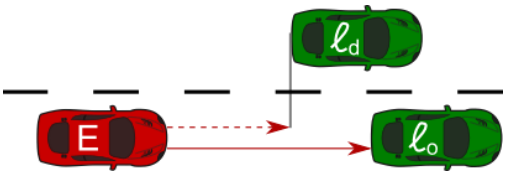

Figure 7 Virtual leader illustration. Solid arrows indicate real leaders, and dashed arrows indicate virtual leaders.

To make this decision, the vehicle considers the desired speeds at the origin and destination lanes. Let the desired speed at the origin lane be:

$$v_o(t) = \begin{cases} V_f, & g_o(t) \geq G \\ v_{\ell o}(t), & g_o(t) < G \end{cases}$$

where V_f is the free-flow speed, $v_{\ell o}(t)$ is the velocity of the origin lane leader, $g_o(t)$ is the gap between the ego vehicle and the origin lane leader, and G is a gap threshold. The desired speed at the destination lane equals the destination lane leader velocity $v_{\ell d}(t)$. Then, we decide to

$$\begin{aligned} \text{overtake } \ell_d, & \quad \text{if } v_o(t) > v_{\ell d}(t) + \delta_v \\ \text{adjust } \ell_d, & \quad \text{otherwise,} \end{aligned}$$

where δ_v is a positive constant. Lower values of δ_v mean the ego vehicle tries to perform overtaking maneuvers that take longer time. If the vehicle decides to merge behind ℓ_d, it must perform longitudinal adjustments that simultaneously keep it at a safe distance from the origin lane leader and create the safe gap to the destination lane leader. To do this, the ego vehicle sets the destination lane leader, ℓ_d, as a virtual leader. A virtual leader is a vehicle that is longitudinally ahead of the ego vehicle, but in a different lane. Conversely, we call real leader the vehicle that is longitudinally ahead of the ego vehicle and on the same lane. This is illustrated in Figure 7. The ego vehicle then computes two desired accelerations: one relative to the real leader, $u_r(t)$, and one relative to the virtual leader, $u_v(t)$. It chooses:

$$u(t) = \min[u_r(t), u_v(t)]$$

as its desired acceleration. This procedure guarantees that the ego vehicle creates a safe gap between itself and ℓ_d while keeping a safe distance to ℓ_o. One should note that, since the ego vehicle and ℓ_d are on different lanes, their initial gap might be very small or even negative. Therefore, differently from a regular longitudinal controller, the virtual following controller must react smoothly in cases of small gaps. We present one possible implementation of a virtual vehicle following controller later on. If there is no destination lane leader, the ego vehicle continues computing its acceleration based on the origin lane leader alone. Periodically, while performing longitudinal adjustments, the ego vehicle has the choice to change the accepted risk value. After that, it checks again whether the gaps satisfy the risk constraint and repeats the decision process. We note that, at any point, the higher-level decision algorithm might decide that there is no more lane change intention, and the ego vehicle will go back to regular lane keeping.

Longitudinal Controllers

We briefly describe the implemented longitudinal controllers. It is important to note that the proposed approach be used with other longitudinal controllers, but we must have a concrete implementation to run simulations. We call “real vehicle following controller” the controller used to keep a safe distance from the vehicle at the origin lane. It is presented for completeness and to help highlight the necessary modifications when dealing with virtual

leaders. We then propose one possible implementation of the virtual vehicle following controller, that is, the controller used to create and keep the desired lane changing gaps.

Real Vehicle Following Controller

For completeness, we present the real vehicle following controller implemented for simulations, which is based on well-known controllers [70, chapter 6] [73]. It is a switched controller that operates either in velocity control mode or in gap control mode based on how far away the real leader is. Mathematically:

$$u_r(t) = \begin{cases} k_1 e_v(t) + k_2 \int_{t_0}^{t} e_v(\tau)\mathrm{d}\tau + k_3 \dot{e}_v(t), & \text{if } g(t) > G(t) \\ k_4 e_g(t) + k_5 e_v(t), & \text{if } g(t) \leq G(t) \end{cases} \quad (9)$$

where $u_r(t)$ is the desired acceleration relative to the real leader, k_i, $i = \{1, \dots, 5\}$ are gains, $e_g(t)$, $e_v(t)$ are the gap and velocity errors respectively, $g(t)$ is the gap to the real leader, and $G(t)$ is a gap threshold. The errors are defined as:

$$e_g(\mathrm{t}) = g(t) - h(r_a)v_E(t) - c, \quad (10)$$

$$e_v(\mathrm{t}) = v_r(t) - v_E(t) \quad (11)$$

where $h(r_a)$ is the time headway that yields a risk of at most r_a, c is a positive constant, $v_E(t)$ and $a_E(t)$ are the ego vehicle's velocity and acceleration respectively. The reference velocity is

$$v_r(t) = \begin{cases} V_f, & \text{if } g(t) > G(t) \\ v_\ell(t), & \text{if } g(t) \leq G(t) \end{cases} \quad (12)$$

where V_f is the free-flow velocity, and $v_\ell(t)$ is the real leader's velocity. The threshold is:

$$G(t) = h(r_a)V_f + c - \frac{k_5}{k_4} e_v(t)$$

which ensures that $u_r(t) \geq 0$ at the transition from velocity to gap control.

Virtual Vehicle Following Controller

In typical longitudinal controllers, the ego vehicle uses a velocity controller when the leader does not exist or when it is far away. If the leader is close, the ego vehicle uses a gap controller to keep the ego vehicle at a desired distance from its leader. If we applied this controller when computing the desired acceleration relative to a virtual leader, the ego vehicle could be subject to an unnecessary strong braking since the initial inter-vehicle gap could be very small or even negative. Therefore, we propose a virtual vehicle following controller where the switching happens in the inverse way. That is, if the gap between the vehicle and its virtual leader is small, the vehicle adopts a velocity controller whose set-point is a fraction of the virtual leader's velocity. This avoids the undesired strong braking, while guaranteeing that the gap between vehicles will increase. When the gap reaches a threshold value, the ego vehicle can switch to gap control and perform finer gap adjustments. We implement it as:

$$u_v(t) = \begin{cases} k_1 e_v(t) + k_2 \int_{t_0}^{t} e_v(\tau)\mathrm{d}\tau + k_3 \dot{e}_v(t), & \text{if } g(t) \le B(t) \\ k_4 e_g(t) + k_5 e_v(t), & \text{if } g(t) > B(t) \end{cases}$$

where $u_v(t)$ is the desired acceleration relative to the virtual leader, k_i, $e_g(t)$ and $e_v(t)$ are as in Eq.(9), $g(t)$ is the gap to the virtual leader, and $B(t)$ is a gap threshold. The reference velocity used to compute $e_v(t)$ is

$$v_r(t) = \begin{cases} \mu v_\ell(t), & \text{if } g(t) \le B(t) \\ v_\ell(t), & \text{if } g(t) > B(t) \end{cases} \quad \textbf{(13)}$$

where $v_\ell(t)$ is the virtual leader's velocity and $0 < \mu < 1$. The threshold is:

$$B(t) = h v_E(t) + c - \frac{k_5}{k_4} e_v(t)$$

which ensures that $u_v(t) = 0$ at the transition from velocity to gap control.

Behavior in Mixed Traffic

Since the autonomous vehicle has no way of detecting whether surrounding vehicles are autonomous or human-driven, it behaves the same way as described above in mixed traffic. If the autonomous vehicle knows it is in an all-autonomous scenario, it can assume surrounding vehicles have low reaction times, thus decreasing the required gap to future followers at the destination lane. If we assume the autonomous vehicles can be visually identified, then the autonomous vehicle with intention to change lanes can take that into consideration when looking for appropriate lane change gaps.

Risk Factors for Connected Vehicles

In this section we propose control algorithms for connected and autonomous vehicles (CAVs) that receive risk as a parameter. The formulas relating risk acceptance to desired time headway and to lane changing gaps are the same as in the previous section. The main difference from AV to CAV is that the latter can communicate and, therefore, cooperate. In what follows, we propose a cooperative lane changing method that can also take an accepted risk value as a parameter. After that, we present the implementation of longitudinal controllers used in the simulations. We end the section with a note on how CAVs behave in mixed traffic.

Risk-Taking in Cooperative Lane Changes

This section presents the control-agnostic cooperative lane changing method that guarantees bounded risk at all times. Moreover, it ensures that suitable lane change gaps at the destination lane are generated thanks to cooperation. As with AVs, we focus on the longitudinal adjustments and on the gap acceptance decision. We assume that, in addition to having the capabilities of an AV, the CAV:

- has access to surrounding vehicles' acceleration, desired time headway, and maximum braking through communications;
- is altruistic, that is, it always cooperates once a cooperation request is received;
- has a free-flow speed $V_f \leq V_{max}$, where V_f is chosen by the vehicle's user, and V_{max} is the maximum legal speed of the road.

The CAV's safe lane changing and longitudinal adjustment decision process is summarized by the flowchart of Figure 8. Compared to the AV flowchart of Figure 6, this one has two extra processes: *Broadcast cooperation request* and *Receive surrounding vehicles' parameters*. The goal of these actions is to inform other vehicles about E's intentions so can then cooperate to generate the gaps that satisfy E's risk constraints. The initial steps are the same: the ego vehicle checks if the current gaps satisfy the risk constraints using conservative assumptions about the surrounding vehicles' braking capabilities. If not, the following two steps are still as in the AV case: we check whether there is a leader in the destination lane and, if yes, whether E should try to overtake it. By design E only tries to overtake ℓ_d if its own desired speed is greater than ℓ_d's speed. Therefore, we expect the overtaking maneuver to happen without any need of cooperation from ℓ_d. If the vehicle decides to merge behind ℓ_d, it must, as in the AV case, set ℓ_d as a virtual leader and perform longitudinal adjustments following Eq. (29). There are two cases in which E requests cooperation (how each surrounding vehicle cooperates is explained in the next paragraph): if there is no destination lane leader, or if E decides to adjust and merge behind the destination lane leader. In both cases, we want to ensure that f_d keeps a longitudinal distance to E that allows E to perform the lane change. If the follower at the destination lane (f_d) exists, it responds by sending back its own desired time headway while ℓ_d responds with its own maximum braking. This allows the ego vehicle to use less conservative estimations of the risks. If we had not assumed that CAVs are altruistic, f_d would also have to reply stating whether it is willing to cooperate. However, the decision problem of when to cooperate is out of the scope of this work.

The three green vehicles illustrated in Figure 9 (f_d, ℓ_d, ℓ_o) cooperate with the lane change maneuver in different ways. The follower at the destination lane (f_d) adopts the lane changing vehicle as a virtual leader as illustrated in Figure 9. In this case, virtual following ensures that the cooperating vehicle creates the desired gap for the lane changing vehicle to move into without compromising the safety between the cooperating vehicle (f_d) and its real leader (ℓ_d). The leader at either the origin (ℓ_o) or destination lane (ℓ_d) cooperates by increasing its free-flow speed to the maximum legal value on the road. Thus, if the cooperating vehicle has no leader, it will accelerate and increase the gap to the lane changing vehicle.

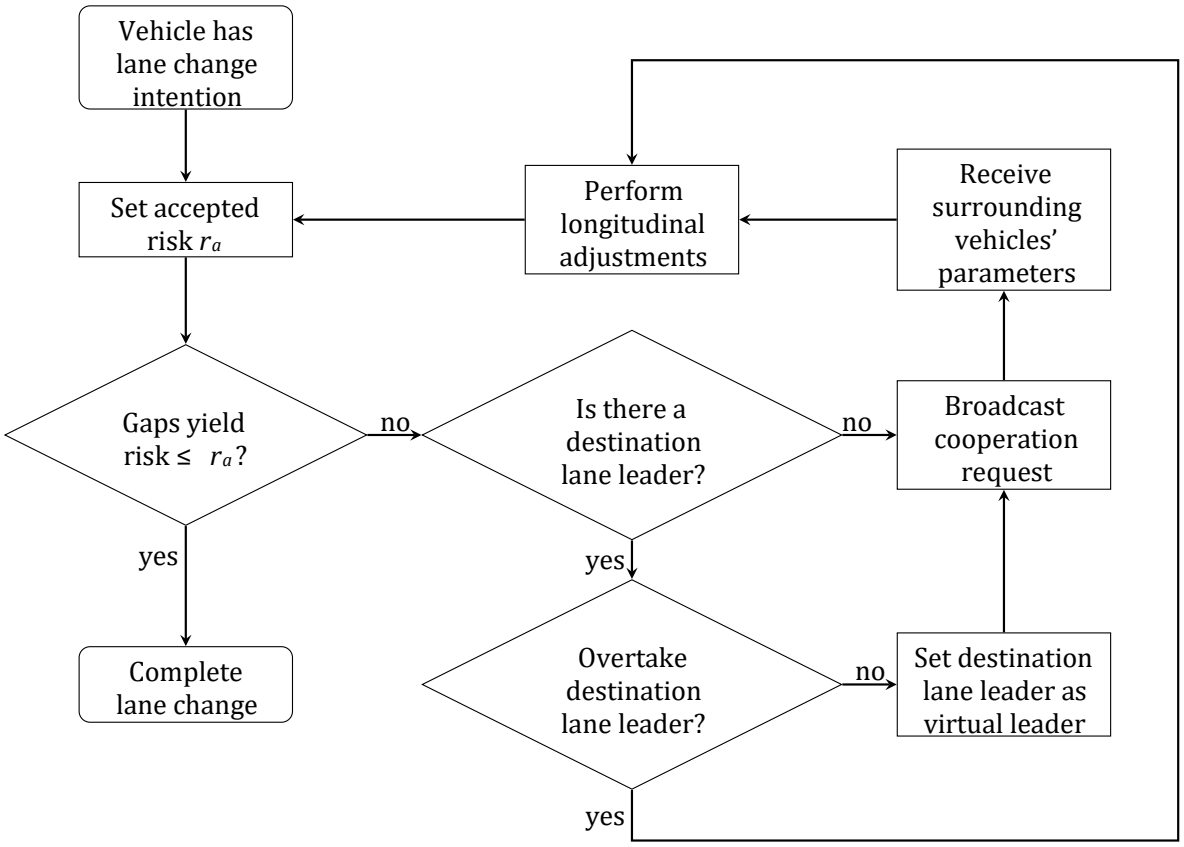

Figure 9 Connected and autonomous vehicle flowchart detailing the lane changing and longitudinal adjustment process.

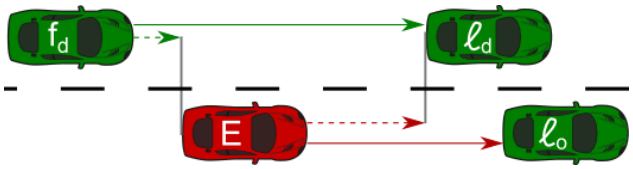

Figure 8 Virtual leader examples. Solid arrows indicate real leaders, and dashed arrows indicate virtual leaders. The vehicle with lane change intention, E, sets the destination lane leader, ℓ_d, as virtual leader while the destination lane follower, f_d, sets E as its virtual leader.

We must address the possibility of a vehicle receiving multiple cooperation requests. There is no conflict if all requests come from vehicles longitudinally behind the cooperating vehicle - it will just keep the maximum legal speed as its free-flow speed. If at least one request comes from a vehicle longitudinally ahead, we ignore requests issued from vehicles longitudinally behind. In other words, the cooperating vehicle chooses the role of destination lane follower over all others. There is also the case where both requests come from vehicles longitudinally ahead, that is, there is one lane changing vehicle ahead to our left and another ahead to our

right. In this situation, the cooperating vehicle adopts two virtual leaders. Consequently, it computes three distinct desired acceleration values and chooses the minimum.

Longitudinal Controllers Implementation

Again, we briefly describe the longitudinal controllers used in simulations for completeness, since other longitudinal controllers could be use together with the proposed approach.

Real Vehicle Following Controller

The real vehicle following controller implemented for simulations is a switched controller that operates either in velocity control mode or in gap control mode based on how far away the real leader is. The main difference from the AV controller is that it can use knowledge about the leading vehicle's acceleration [74]. Moreover, thanks to communications, a CAV can make less conservative assumptions about the leading vehicles braking capabilities, which leads to smaller time headway values when compared to AVs. The controller is:

$$u_r(t) = \begin{cases} k_1 e_v(t) + k_2 \int_{t_0}^{t} e_v(\tau)\mathrm{d}\tau + k_3 \dot{e}_v(t), & \text{if } g(t) > G(t) \\ k_4 e_g(t) + k_5 \dot{e}_g(t) + k_6 e_v(t) + k_7 e_a(t), & \text{if } g(t) \leq G(t) \end{cases} \quad \textbf{(14)}$$

where $u_r(t)$ is the desired acceleration relative to the real leader, k_i, $i = \{1, \dots, 7\}$ are gains, $e_g(t)$, $e_v(t)$ and $e_a(t)$ are the gap, velocity and acceleration errors respectively, $g(t)$ is the gap to the real leader, and $G(t)$ is a gap threshold. The gap and velocity errors are as in (10) and (11 **)** respectively, and

$$e_a(t) \quad = \dot{v}_r(t) - a_E(t)$$

where $v_r(t)$ is the reference speed defined in (12), and $a_E(t)$ is the ego vehicle's acceleration respectively. The threshold is:

$$G(t) = hV_f + c - \frac{1}{k_4}\left(k_5 \dot{e}_g(t) + k_6 e_v(t) + k_7 e_a(t)\right)$$

which ensures that $u_r(t) \geq 0$ at the transition from velocity to gap control.

Virtual Vehicle Following Controller

As in the AV controllers, we need a virtual vehicle following controller that ensures smooth gap increase even if the initial gap is close to zero. Therefore, we follow a similar approach to define the CAV virtual vehicle following controller. We implement it as:

$$u_v(t) = \begin{cases} k_1 e_v(t) + k_2 \int_{t_0}^{t} e_v(\tau)\mathrm{d}\tau + k_3 \dot{e}_v(t), & \text{if } g(t) \leq B(t) \\ k_4 e_g(t) + k_5 \dot{e}_g(t) + k_6 e_v(t) + k_7 e_a(t), & \text{if } g(t) > B(t) \end{cases}$$

where $u_v(t)$ is the desired acceleration relative to the virtual leader, k_i, $e_g(t)$, $e_v(t)$ and $e_a(t)$ are as in Eq. (14), $g(t)$ is the gap to the virtual leader, and $B(t)$ is a gap threshold. The reference velocity used to compute $e_v(t)$ is as in (13). The threshold is:

$$B(t) = hv_E(t) + c - \frac{1}{k_4}\left(k_5\dot{e}_g(t) + k_6 e_v(t) + k_7 e_a(t)\right)$$

which ensures that $u_v(t) = 0$ at the transition from velocity to gap control.

Behavior in Mixed Traffic

We assume that a CAV periodically broadcasts messages looking for other connected vehicles in its surroundings. While the connected vehicle does not identify any other connected vehicle around, it behaves as an autonomous vehicle. If a connected vehicle is following another connected vehicle, it can adopt a smaller reference gap and use the control law in (14). When changing lanes, if the CAV does not receive replies from the surrounding vehicles, it follows the AV behavior outlined in the flowchart of Figure 6.

Safety/Efficiency Trade-Off Evaluations

Simulator and Evaluation Metrics

We use PTV's traffic simulator VISSIM to evaluate how the proposed algorithms affect traffic flow and safety on a highway. We let VISSIM's own algorithm dictate the behavior of human drivers (see [75] for details). The software allows users to define vehicle behaviors through a C++ coded Dynamic Linked Library (DLL). We make use of this to implement our method. As stated before, our focus is not on lane choice, so VISSIM decides if a vehicle has lane change intention. From VISSIM output files, we compute the highway input flow at every $30\ s$, and we compute the instantaneous risk for each vehicle at every $0.1\ s$. To evaluate safety, we count the number of risky intervals with risk greater than 1. Moreover, we compute the risk R_i of each risky interval and the total risk of each simulation. The described simulation framework is summarized in Figure 10.

We create a challenging scenario where lots of lane changes must happen in a relatively short stretch of a highway that allows us to evaluate the performance of AVs and CAVs at different levels of congestion and obtain insights on the safety vs. traffic flow trade-off as we vary the values of accepted risk. The scenario, illustrated in Figure 11, is composed of a 2-lane highway with an in ramp and an off ramp. Vehicles trying to merge into the highway or to take the off ramp have $500m$ to do so. Vehicles that start on the highway's left lane, stay on the highway. They can end the simulation at either one of the highway lanes. 10% of vehicles that start on the highway's right lane take the off ramp, and all vehicles that start on the in-ramp merge into the highway. We measure the traffic flow at the start of the merging segment.

We evaluate each studied scenario in terms of efficiency and safety. Efficiency is measured by two variables: completed lane changes and traffic flow. As described in section 3, we measure safety by counting the number of risky lane changes and by computing the median risk value of the risky lane changes.

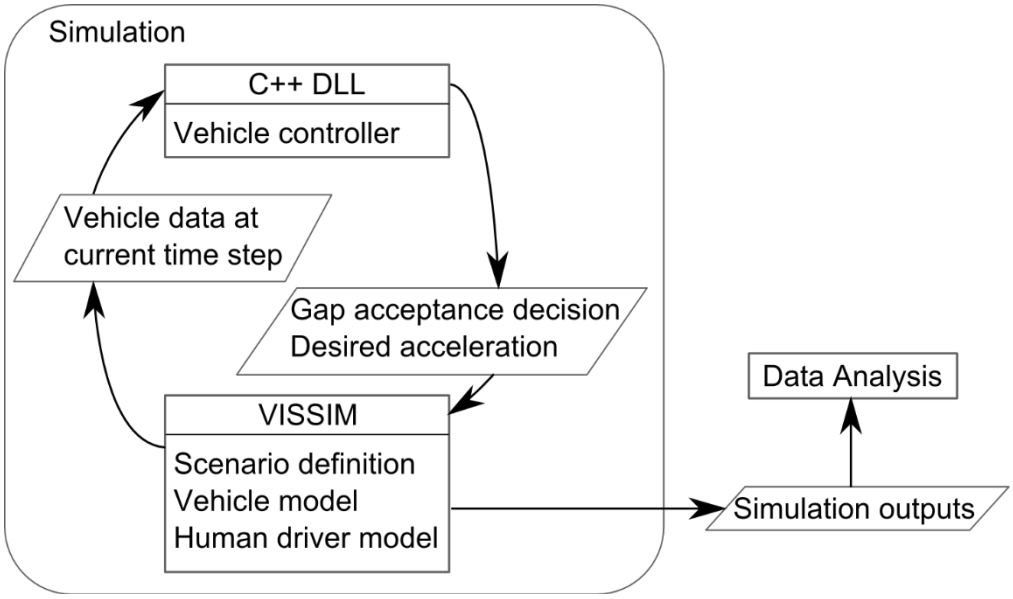

Figure 11 Simulation set-up: VISSIM simulates vehicles on the highway, the DLL controls AVs and CAVs, and a separate code evaluates the simulation results after they finish.

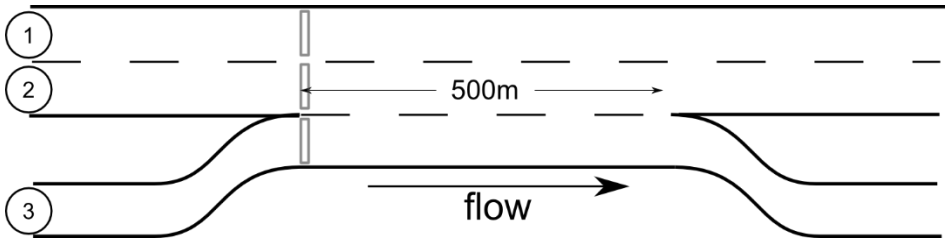

Figure 10 The vehicle flow is from the left to the right. All vehicles that start on lane 1 stay on the highway, 10% of vehicles that start on lane 2 take the off ramp, and all vehicles that start lane 3 move into the highway. Vehicle counting sensors are indicated by gray vertical rectangles.

Experiment 1: uniform vehicle fleets

In the first set of experiments, we assume that all the vehicles in the simulation are either:

1. Human driven vehicle (HDV): vehicle behavior is dictated entirely by VISSIM.
2. Autonomous Vehicle (AV): the vehicle's behavior is as described in section 4. Moreover, if a vehicle is stopped waiting for a suitable lane change gap for over $45\ s$, we give control back to VISSIM. This is similar to having an autonomous vehicle request the driver to take over when it does not know what to do.
3. Connected and Autonomous Vehicle (CAV): the vehicle behavior is as described in section 5. In this case, the cooperative behavior guarantees no vehicle gets "stuck"

waiting for an appropriate lane change gap, so there is no need to hand control back to VISSIM in any case.

To compare uncongested and congested cases, we run 30-minute simulations with inputs of 1000 and 2000 vehicles per lane per hour. To analyze the effects of risk acceptance, we define risk categories as in Table 2 in the simulations which contain AVs or CAVs. Therefore, there are 18 scenarios, each of which is run 10 times to account for the randomness of traffic simulations. The results are summarized in Table 3 and Table 4. We highlight that the accepted risk is used in the computation of the accepted lane change gaps, which, by design, overestimates the actual risk. The number of risk lane changes and the median risk per lane change our computed using the exact risk formulas, i.e., Eqs. (7) and (8).

The safety metrics are further detailed in (a) (b) (c) (d) (e) (f) (g) (h)

Figure 12, which shows histograms of the total lane change risk for human driven vehicles ((a) (b) (c) (d) (e) (f) (g) (h)

Figure 12b), for AVs with varying values of accepted risk ((a) (b) (c) (d) (e) (f) (g) (h)

Figure 12 a, c, e, g), and CAVs with varying values for accepted risks ((a) (b) (c) (d) (e) (f) (g) (h)

Figure 12 d, f, h). We do not show the case of CAVs with zero accepted risk because this scenario does not create any risky lane changes. The flow results are further detailed in the box plots of

(a)

(b)

Figure 13. In a box plot the four quartiles of the data can be quickly identified. The two middle quartiles (from 25% to 75% of the data) are indicated by a colored box, and the whiskers represent the minimum and maximum values except for outliers, which are displayed as diamonds.

Table 2 Risk Categories

Category	Accepted collision severity in the worst-case scenario (km/h)
Safe	0
Low	36
Medium	72
High	108

Table 3 Lane Change Risks and Flow Results at 3000 Vehicles per Hour

Vehicle type	Risk Category	Mean number of risky lane changes	Median lane change risk (*m*)	Median flow (vehs/h)	Completed lane changes
HDV	-	417	33	2880	569
AV	Safe	1.6	3.3	2640	190
	Low	1.9	8.4	2880	536
	Medium	293	5.1	2880	1039
	High	433	7.2	2880	1248
CAV	Safe	0	0	3000	539
	Low	0.1	0.55	3000	933
	Medium	185	3.5	2880	1309
	High	258	3.7	2880	1423

Table 4 Lane Change Risks and Flow Results at 6000 Vehicles per Hour

Vehicle type	Risk Category	Mean number of risky lane changes	Median lane change risk (*m*)	Median flow (vehs/h)	Completed lane changes
HDV	-	526	7	4080	810
AV	Safe	0.11	1.0	4440	155
	Low	1.1	1.5	4680	185
	Medium	34	2.4	4440	329
	High	37	1.9	4440	351
CAV	Safe	0	0	4680	394
	Low	0.2	13	4680	434
	Medium	54	7.7	4800	480
	High	52	10	4800	481

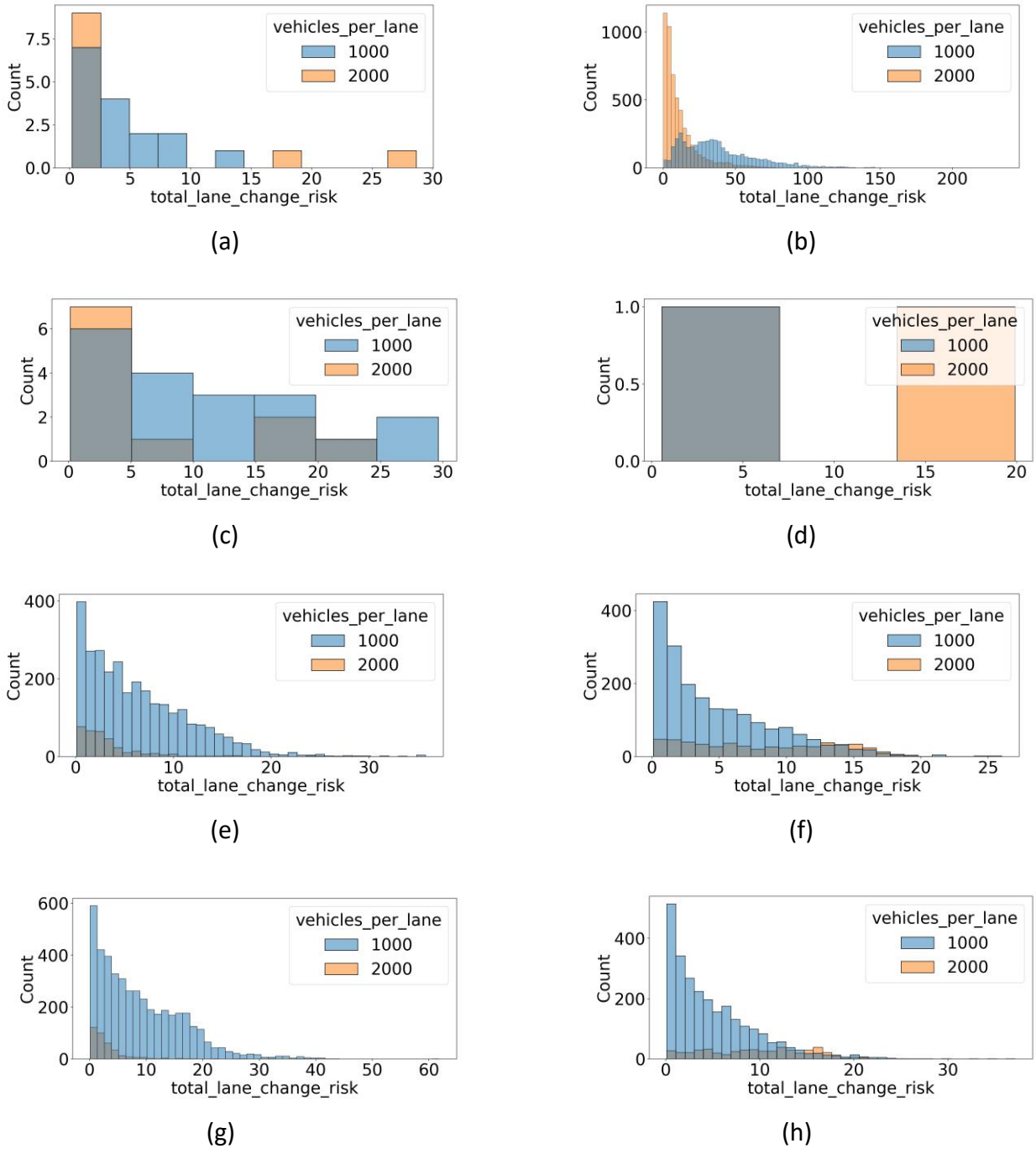

Figure 12 Risks of lane changes for human driven vehicles, and for AVs and CAVs with varying accepted risk values. Parameters of each figure are: (a) 100% AV, safe, (b) 100% human driven, (c) 100% AV, low risk, (d) 100% CAV, low risk, (e) 100% AV, medium risk, (f) 100% CAV, medium risk, (g) 100% AV, high risk, (h) 100% CAV, high risk.

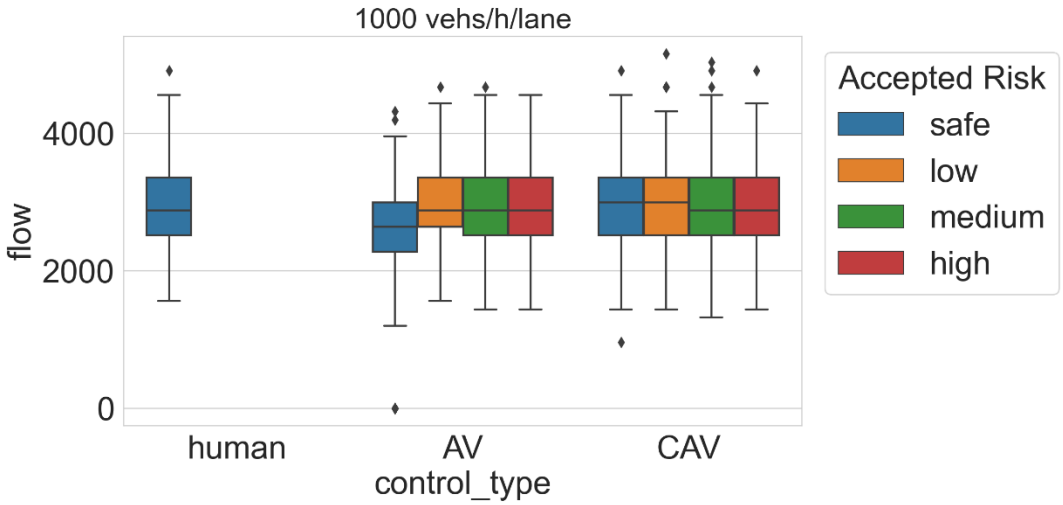

(c)

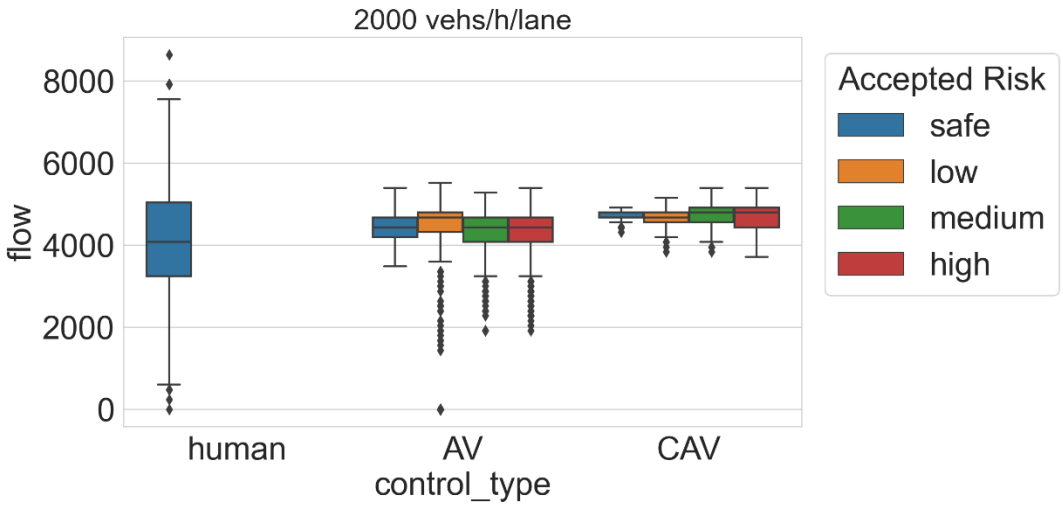

(d)

Figure 13 Distribution of traffic flow measurements for each scenario. The colored boxes contain 50% of the data that is closest to the median value. The whiskers represent the minimum and maximum values except for outliers, which are represented by black diamonds. In (a), the total vehicle input is 3000 vehicles per hour. In (b), the total vehicle input is 6000 vehicles per hour.

Let us start by evaluating the safety of human driving. Regarding flows, the median value of 2880 in the scenarios with input of 3000 vehicles per hour confirms the absence of congestion in this case. Similarly, the median flow of 4080 in the simulations with 6000 vehicles per hour confirm that there is congestion. Regarding the safety evaluation, it is important to remember that our risk was defined to be zero only when it is possible to avoid collision under the worst-case braking scenario. Moreover, we take into consideration the reduced braking capabilities of the vehicles during lateral maneuver. Therefore, it is not surprising that that most of the lane changes completed by human drivers produced some risk (73% and 64% on the uncongested and congested scenarios respectively). It is interesting to note that the median risk in the congested scenario is much lower than in the uncongested scenario. This happens because, in the congested scenario, the vehicles are traveling at slower velocities and the relative velocity between lanes is also smaller, which creates less high-risk situations. This result agrees with previous findings [76].

Next let us evaluate the safety/ efficiency trade-off of autonomous vehicles. It is clear that AVs that take no risks are, as expected, much safer than human driven vehicles. The few risky lane changes are caused when two vehicles decide to move into the same lane (one coming from the right and the other from the left) at the exact same simulation time step. Since we are not considering evasive maneuvers in this work, when this happens, they both proceed with their maneuvers and may end up at close distance from one another. The increased safety comes at a clear cost in efficiency in the uncongested scenario. When the AV does not take any risk in a scenario where there might be high relative velocity between lanes, it sometimes gets stuck in a lane. This causes some congestion on that lane, which is then reflected by the lower median flow. In the congested case, this effect is not seen. In a congestion, relative velocities between lanes are smaller, making it easier for the AV to perform lane changes. More importantly, as can be seen be the flow variance in the box plot of

(e)

(f)

Figure 13b, human driven vehicles lead to stop and go behavior, which is prejudicial for the flow. Since the AVs are equipped with controllers that are string-stable, they lead to a more constant flow.

As soon as the AVs accept low risks, there is no more flow decrease in the uncongested scenario. Furthermore, the number of completed lane changes also gets close to the case of human driven vehicles. It is interesting to note that, at the low risk, the number of risky lane changes is still close to zero (it is below 1% of the completed lane changes). This confirms that the safe category is indeed very conservative. On the other hand, increasing the accepted risk leads to significantly more risky maneuvers without any gain in flow. The number of completed lane changes also increases sharply (it almost doubles from low to medium risk). This value is driven by discretionary lane changes, that is, vehicles trying to move to a faster moving lane. We also note that, as is the case with human drivers, the median lane change risk is much higher in the uncongested scenario.

We can see CAVs are in general safer than AVs even when both accept the same risk value. This occurs because CAVs can better estimate risks thanks to communication. Moreover, thanks to cooperation, the CAVs always lead to equal or higher flow than both human driven and autonomous vehicles. The CAV's extended capabilities also mean that there is not much room for efficiency improvement by accepting risks. In the uncongested case, the median flow actually decreases at higher accepted risk values. This happens because vehicles that cut in force others to decelerate, which negatively impacts flow.

Given that it will take a considerable amount of time for all vehicles to be automated, the second set of simulations evaluates the impacts of varying penetration levels of AVs and CAVs on the same scenarios.

Experiment 2: mixed traffic

We now focus on the effects of AVs and CAVs in mixed traffic. To do that, we vary the penetration of AVs and CAVs by increments of 25%. Analysis of the results of experiment 1 showed that AVs and CAVs perform better than humans in the congested scenario even without taking any risks. Moreover, we noticed that accepting the highest value of risk did not bring any noticeable advantages. Therefore, we choose to focus on the uncongested scenario, and we only simulate zero, low and medium accepted risks. The safety and efficiency results are summarized in Table 5. We repeated the results from uniform fleets, i.e., all human driven vehicles (HDVs), all AVs and all CAVs, for easier comparison. The more detailed safety results are shown in the histograms of

(a) (b)
(c) (d)
(e) (f)
(g) (h)

Figure 14.

At low penetrations, AVs and CAVs working at all risk levels increase the number of risky lane changes when compared to the 100% HDVs case by around 30%. At the same time, the median lane change risk decreases by a smaller margin (between 6% and 12%). We also see that the number of completed lane changes increases considerably from 569 to more than 800. We conclude that the percentage of risky lane changes among the total completed lane changes actually decreases from 73% to around 65%. Upon further examination, we find that from 90% to 99% of the risky maneuvers when the AVs and CAVs are in the safe category come from human driven vehicles. After looking at simulation videos, we see that the conservative behavior of AVs and CAVs when looking for gaps makes HDVs perform more lane changes for two reasons. First, AVs and CAVs smoothly brake when looking for gaps. HDVs following these AVs or CAVs might see that the neighboring lane is traveling faster and, without being restricted by the same safety rules, change lanes before the AV or CAV. At the same time, when looking for gaps, the AVs and CAVs tend to create large gaps ahead of them, which are also used by HDVs. As the penetration levels increase, the risk acceptance starts having bigger impacts in the results. However, we still see a big gap from the results with 75% penetration of either AV or CAV and 100% penetration. These results imply that small numbers of AVs and CAVs do not

bring significant advantages to the general traffic, and that the main benefits are only reaped at full automation. This conclusion should be taken with a grain of salt, since VISSIM's model of human drivers is only calibrated to interact with other human drivers.

Table 5 Lane Change Risks and Flow Results at 3000 Vehicles per Hour and Varying AV and CAV Penetration

Fleet composition	Risk Category	Mean number of risky lane changes	Median lane change risk (*m*)	Median flow (vehs/h)	Completed lane changes
100% HDV	-	417	33	2880	569
25% AV	Safe	536	31	2880	827
	Low	541	30	2880	838
	Medium	542	29	2880	825
50% AV	Safe	360	28	2880	641
	Low	406	27	2880	768
	Medium	486	22	2880	860
75% AV	Safe	201	22	2880	494
	Low	209	23	2880	632
	Medium	394	13	2880	894
100% AV	Safe	1.6	3.3	2640	190
	Low	1.9	8.4	2880	536
	Medium	293	5.1	2880	1039
25% CAV	Safe	544	30	2880	837
	Low	523	31	2880	819
	Medium	547	29	2880	815
50% CAV	Safe	499	25	2880	946
	Low	504	27	2880	1005
	Medium	642	22	2880	1106
75% CAV	Safe	279	18	2880	803
	Low	307	18	3000	1015
	Medium	628	13	2880	1408
100% CAV	Safe	0	0	3000	539
	Low	0.1	0.55	3000	933
	Medium	195	3.5	2880	1309

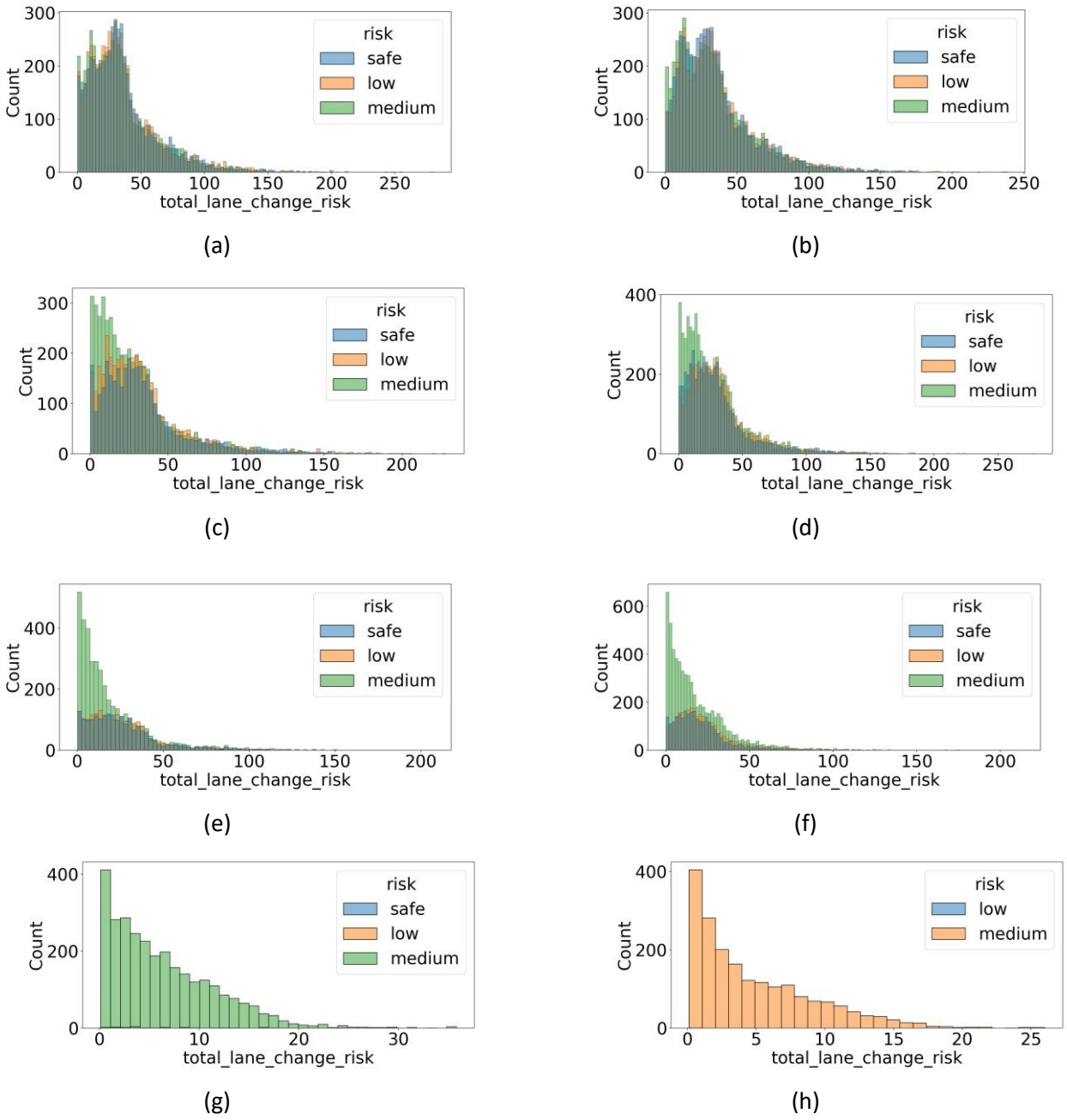

Figure 14 Risks of lane changes for varying penetrations of AVs and CAVs. To the left, mixed traffic of humans and AVs with penetrations of 25%, 50%, 75% and 100% in plots (a), (c), (e) and (g) respectively. To the right, mixed traffic of humans and CAVs with penetrations of 25%, 50%, 75% and 100% in plots (b), (d), (f) and (h) respectively.

Conclusion

In this work we have studied the trade-off between safety and efficiency of AVs and CAVs in highways with mixed traffic. We defined a risk assessment metric that considers both the severity of a collision that would happens under a worst-case braking scenario and the time the vehicle is exposed to a possible collision. We use this metric, together with the concept of virtual vehicles, in an approach for lane changing longitudinal adjustments and gap acceptance. This method can be used to ensure that the AV is never in a collision prone situation. Moreover, the proposed method can take risk as a parameter so that the AV behaves less conservatively if that is desired. We then extended this approach to CAVs, which can make use of communications to request that vehicles in the destination lane cooperate to generate acceptable lane change gaps.

We studied our proposed approaches through extensive simulations. We analyzed how different factors impact safety, measured by the number of risky lane changes and their median risk, and efficiency, measured by the number of completed lane changes and traffic flow. We varied the number of vehicles entering the network, the types of vehicles and their penetration percentages as well as the accepted risks. Our mains conclusions are:

- AVs can be too conservative, which negatively impacts flow. However, accepting low risks makes a fleet made only of AVs as efficient as the human driven fleet.
- The cooperation used by CAVs allow this type of vehicle to improve both safety and efficient simultaneously.
- The biggest challenge lies in mixed traffic. At low penetrations, both AVs and CAVs behave safely around humans, but they do not have a significant impact on macroscopic metrics.

The last conclusion indicates two important directions of research. The first is the modeling of how humans will behave around AVs and CAVs. Since we know that micro simulators such as VISSIM are not calibrated for this scenario, the simulation results may not accurately reflect reality. The second is the design of AVs and CAVs that are not only safe, but that also help human drivers behave more safely.

References

[1] U. D. of Transportation, "Automated vehicles 3.0: Preparing for the future of transportation," 2018.

[2] A. Talebpour and H. S. Mahmassani, "Influence of connected and autonomous vehicles on traffic flow stability and throughput," *Transportation Research Part C: Emerging Technologies*, vol. 71, pp. 143–163, oct 2016.

[3] D. Desiraju, T. Chantem, and K. Heaslip, "Minimizing the disruption of traffic flow of automated vehicles during lane changes," *IEEE Transactions on Intelligent Transportation Systems*, vol. 16, pp. 1249–1258, 2015.

[4] J. Rios-Torres and A. A. Malikopoulos, "A Survey on the Coordination of Connected and Automated Vehicles at Intersections and Merging at Highway On-Ramps," *IEEE Transactions on Intelligent Transportation Systems*, vol. 18, no. 5, pp. 1066–1077, 2017.

[5] R. Ammourah and A. Talebpour, "Deep reinforcement learning approach for automated vehicle mandatory lane changing," *Transportation Research Record: Journal of the Transportation Research Board*, p. 036119812211083, 7 2022.

[6] S. Lefevre, D. Vasquez, and C. Laugier, "A survey on motion prediction and risk assessment` for intelligent vehicles," *ROBOMECH Journal*, vol. 1, no. 1, pp. 1–14, 2014.

[7] H. Yu, R. Jiang, Z. He, Z. Zheng, L. Li, R. Liu, and X. Chen, "Automated vehicle-involved traffic flow studies: A survey of assumptions, models, speculations, and perspectives," *Transportation Research Part C: Emerging Technologies*, vol. 127, no. April, 2021.

[8] Y. Li, Y. Zheng, B. Morys, S. Pan, J. Wang, and K. Li, "Threat Assessment Techniques in Intelligent Vehicles: A Comparative Survey," *IEEE Intelligent Transportation Systems Magazine*, no. January 2020, 2020.

[9] S. M. Mahmud, L. Ferreira, M. S. Hoque, and A. Tavassoli, "Application of proximal surrogate indicators for safety evaluation: A review of recent developments and research needs," *IATSS Research*, vol. 41, no. 4, pp. 153–163, 2017.

[10] J. C. Hayward, "Near-miss determination through," *Highway Research Board*, pp. 24–35, 1972.

[11] E. Coelingh, A. Eidehall, and M. Bengtsson, "Collision warning with full auto brake and pedestrian detection - A practical example of automatic emergency braking," *IEEE Conference on Intelligent Transportation Systems, Proceedings, ITSC*, pp. 155–160, 2010.

[12] M. M. Minderhoud and P. H. Bovy, "Extended time-to-collision measures for road traffic safety assessment," *Accident Analysis and Prevention*, vol. 33, no. 1, pp. 89–97, 2001.

[13] A. Laureshyn, T. D. Ceunynck, C. Karlsson, Ase Svensson, and S. Daniels, "In search of the˚ severity dimension of traffic events: Extended delta-v as a traffic conflict indicator," *Accident Analysis and Prevention*, vol. 98, pp. 46–56, 1 2017.

[14] S. G. Shelby, "Delta-v as a measure of traffic conflict severity," 9 2011.

[15] K. Vogel, "A comparison of headway and time to collision as safety indicators," *Accident Analysis and Prevention*, vol. 35, no. 3, pp. 427–433, 2003.

[16] R. Rajamani and S. Shladover, "An experimental comparative study of autonomous and co-operative vehicle-follower control systems," *Transportation Research Part C: Emerging Technologies*, vol. 9, no. 1, pp. 15–31, feb 2001.

[17] S. Darbha, S. Konduri, and P. R. Pagilla, "Benefits of V2V Communication for Autonomous and Connected Vehicles," *IEEE Transactions on Intelligent Transportation Systems*, vol. 20, no. 5, pp. 1954–1963, may 2019.
[18] F. V. Monteiro and P. Ioannou, "Safe Lane Change and Merging Gaps in Connected Environments (in press)," in *Control in Transportation Systems*. Lille, France: IFAC, 2021.
[19] S. Almqvist, C. Hyden, and R. Risser, "Use of speed limiters in cars for increased safety and a better environment," *Transportation Research Record*, no. 1318, 1991.
[20] C. Y. Chan, "Defining safety performance measures of driver-assistance systems for intersection left-turn conflicts," 2006, pp. 25–30.
[21] F. Cunto, "Assessing safety performance of transportation systems using microscopic simulation," p. 190, 2008.
[22] C. Xu, W. Zhao, and C. Wang, "An integrated threat assessment algorithm for decisionmaking of autonomous driving vehicles," *IEEE Transactions on Intelligent Transportation Systems*, vol. 21, pp. 2510–2521, 6 2020.
[23] X. Zheng, B. Huang, D. Ni, and Q. Xu, "A novel intelligent vehicle risk assessment method combined with multi-sensor fusion in dense traffic environment," *Journal of Intelligent and Connected Vehicles*, vol. 1, pp. 41–54, 12 2018.
[24] L. Zhang, W. Xiao, Z. Zhang, and D. Meng, "Surrounding vehicles motion prediction for risk assessment and motion planning of autonomous vehicle in highway scenarios," *IEEE Access*, 2020.
[25] H. C. Joksch, "Velocity change and fatality risk in a crash—a rule of thumb," *Accident Analysis and Prevention*, vol. 25, pp. 103–104, 2 1993.
[26] D. J. Gabauer and H. C. Gabler, "Comparison of roadside crash injury metrics using event data recorders," *Accident Analysis and Prevention*, vol. 40, pp. 548–558, 3 2008.
[27] N. S. Johnson and H. C. Gabler, "Accuracy of a Damage-Based Reconstruction Method in NHTSA Side Crash Tests," *Traffic Injury Prevention*, vol. 13, no. 1, pp. 72–80, 2012.
[28] R. M. Brach and R. M. Brach, "A review of impact models for vehicle collision," *SAE Transactions*, vol. 96, pp. 175–190, 1987.
[29] H. Jula, E. Kosmatopoulos, and P. Ioannou, "Collision avoidance analysis for lane changing and merging," *IEEE Transactions on Vehicular Technology*, vol. 49, no. 6, pp. 2295–2308, 2000.
[30] A. Kanaris, E. Kosmatopoulos, and P. Loannou, "Strategies and spacing requirements for lane changing and merging in automated highway systems," *IEEE Transactions on Vehicular Technology*, vol. 50, no. 6, pp. 1568–1581, 2001.
[31] H. C.-H. Hsu and A. Liu, "Kinematic design for platoon-lane-change maneuvers," *IEEE Transactions on Intelligent Transportation Systems*, vol. 9, no. 1, pp. 185–190, 2008.
[32] Y. Luo, G. Yang, M. Xu, Z. Qin, and K. Li, "Cooperative Lane-Change Maneuver for Multiple Automated Vehicles on a Highway," *Automotive Innovation*, vol. 2, no. 3, pp. 157–168, 2019.
[33] M. Xu, Y. Luo, G. Yang, W. Kong, and K. Li, "Dynamic Cooperative Automated LaneChange Maneuver Based on Minimum Safety Spacing Model *," *2019 IEEE Intelligent Transportation Systems Conference (ITSC)*, pp. 1537–1544, 2019.

[34] R. Chandra, Y. Selvaraj, M. Brannstr¨ om, R. Kianfar, and N. Murgovski, "Safe autonomous¨ lane changes in dense traffic," *IEEE Conference on Intelligent Transportation Systems, Proceedings, ITSC*, vol. 2018-March, pp. 1–6, 2018.

[35] A. Kesting, M. Treiber, and D. Helbing, "General Lane-Changing Model MOBIL for CarFollowing Models," *Transportation Research Record: Journal of the Transportation Research Board*, vol. 1999, no. 1, pp. 86–94, jan 2007.

[36] S. Ulbrich and M. Maurer, "Towards Tactical Lane Change Behavior Planning for Automated Vehicles," in *2015 IEEE 18th International Conference on Intelligent Transportation Systems*, vol. 2015-Octob. IEEE, sep 2015, pp. 975–981.

[37] R. Schubert, K. Schulze, and G. Wanielik, "Situation assessment for automatic lane-change maneuvers," *IEEE Transactions on Intelligent Transportation Systems*, vol. 11, no. 3, pp. 607–616, 2010.

[38] Y. L. Morgan, "Notes on DSRC & WAVE Standards Suite: Its Architecture, Design, and Characteristics," *IEEE Communications Surveys and Tutorials*, vol. 12, no. 4, pp. 504–518, 2010.

[39] J. Rios-Torres and A. A. Malikopoulos, "Automated and Cooperative Vehicle Merging at Highway On-Ramps," *IEEE Transactions on Intelligent Transportation Systems*, vol. 18, no. 4, pp. 780–789, apr 2017.

[40] A. Uno, T. Sakaguchi, and S. Tsugawa, "A merging control algorithm based on inter-vehicle communication," *Proceedings 199 IEEE/IEEJ/JSAI International Conference on Intelligent Transportation Systems*, pp. 783–787, 1999.

[41] H. Liu, W. Zhuang, G. Yin, Z. Tang, and L. Xu, "Strategy for heterogeneous vehicular platoons merging in automated highway system," *Proceedings of the 30th Chinese Control and Decision Conference, CCDC 2018*, pp. 2736–2740, 2018.

[42] K. Raboy, J. Ma, E. Leslie, F. Zhou, K. Rush, and J. Stark, "A Proof-Of-Concept Field Experiment on Cooperative Control for Lane Change Maneuvers with New Connected and Automated Vehicle Technologies," *Transportation Research Board 96th Annual Meeting*, pp. 1–10, 2017.

[43] K. Raboy, J. Ma, E. Leslie, and F. Zhou, "A proof-of-concept field experiment on cooperative lane change maneuvers using a prototype connected automated vehicle testing platform," *Journal of Intelligent Transportation Systems*, vol. 0, no. 0, pp. 1–16, jun 2020.

[44] T. C. D. Santos and D. F. Wolf, "Bargaining game approach for lane change maneuvers," *2019 19th International Conference on Advanced Robotics, ICAR 2019*, pp. 629–634, 2019.

[45] E. Semsar-Kazerooni, K. Elferink, J. Ploeg, and H. Nijmeijer, "Multi-objective platoon maneuvering using artificial potential fields," *IFAC-PapersOnLine*, vol. 50, no. 1, pp. 15006– 15011, jul 2017.

[46] G. An and A. Talebpour, "Lane-Changing Trajectory Optimization to Minimize Traffic Flow Disturbance in a Connected Automated Driving Environment," *2019 IEEE Intelligent Transportation Systems Conference, ITSC 2019*, pp. 1794–1799, 2019.

[47] A. Arun, M. M. Haque, A. Bhaskar, S. Washington, and T. Sayed, "A systematic mapping review of surrogate safety assessment using traffic conflict techniques," *Accident Analysis and Prevention*, vol. 153, no. June 2020, p. 106016, 2021.

[48] M. Wang, W. Daamen, S. P. Hoogendoorn, and B. van Arem, "Rolling horizon control framework for driver assistance systems. part ii: Cooperative sensing and cooperative control," *Transportation Research Part C: Emerging Technologies*, vol. 40, pp. 290–311, 3 2014.

[49] M. Wang, S. P. Hoogendoorn, W. Daamen, B. van Arem, and R. Happee, "Game theoretic approach for predictive lane-changing and car-following control," *Transportation Research Part C: Emerging Technologies*, vol. 58, pp. 73–92, sep 2015.

[50] H. Yu, H. E. Tseng, and R. Langari, "A human-like game theory-based controller for automatic lane changing," *Transportation Research Part C: Emerging Technologies*, vol. 88, no.
February, pp. 140–158, 2018.

[51] H. Wang, S. Xu, and L. Deng, "Automatic lane-changing decision based on single-step dynamic game with incomplete information and collision-free path planning," *Actuators*, vol. 10, 2021.

[52] Y. Wang, H. Deng, and G. Chen, "Lane-change gaming decision control based on multiple targets evaluation for autonomous vehicle," *Transportation Research Record: Journal of the Transportation Research Board*, p. 036119812110111, 2021.

[53] M. Khonji, J. Dias, R. Alyassi, F. Almaskari, and L. Seneviratne, "A risk-aware architecture for autonomous vehicle operation under uncertainty." Institute of Electrical and Electronics Engineers Inc., 11 2020, pp. 311–317.

[54] S. Sohrabi, A. Khodadadi, S. M. Mousavi, B. Dadashova, and D. Lord, "Quantifying the automated vehicle safety performance: A scoping review of the literature, evaluation of methods, and directions for future research," *Accident Analysis and Prevention*, vol. 152, no. October 2020, p. 106003, 2021.

[55] A. D. Tibljas, T. Giuffr˘ e, S. Surdonja, and S. Trubia, "Introduction of Autonomous Vehi-` cles: Roundabouts design and safety performance evaluation," *Sustainability (Switzerland)*, vol. 10, no. 4, pp. 1–14, 2018.

[56] S. M. Mousavi, O. A. Osman, D. Lord, K. K. Dixon, and B. Dadashova, "Investigating the safety and operational benefits of mixed traffic environments with different automated vehicle market penetration rates in the proximity of a driveway on an urban arterial," *Accident Analysis and Prevention*, vol. 152, no. July 2020, p. 105982, 2021.

[57] R. Arvin, A. J. Khattak, M. Kamrani, and J. Rio-Torres, "Safety evaluation of connected and automated vehicles in mixed traffic with conventional vehicles at intersections," *Journal of Intelligent Transportation Systems: Technology, Planning, and Operations*, vol. 25, pp. 170–187, 2020.

[58] Y. Li, H. Wang, W. Wang, L. Xing, S. Liu, and X. Wei, "Evaluation of the impacts of cooperative adaptive cruise control on reducing rear-end collision risks on freeways," *Accident Analysis and Prevention*, vol. 98, pp. 87–95, 2017.

[59] L. Ye and T. Yamamoto, "Evaluating the impact of connected and autonomous vehicles on traffic safety," *Physica A: Statistical Mechanics and its Applications*, vol. 526, p. 121009, 2019.

[60] B. Wang, W. Li, H. Wen, and X. Hu, "Modeling impacts of driving automation system on mixed traffic flow at off-ramp freeway facilities," *Physica A: Statistical Mechanics and its Applications*, vol. 573, p. 125852, 2021.

[61] M. Bahram, Z. Ghandeharioun, P. Zahn, M. Baur, W. Huber, and F. Busch, "Microscopic traffic simulation based evaluation of highly automated driving on highways," *2014 17th IEEE International Conference on Intelligent Transportation Systems, ITSC 2014*, pp. 1752–1757, 2014.

[62] A. Papadoulis, M. Quddus, and M. Imprialou, "Evaluating the safety impact of connected and autonomous vehicles on motorways," *Accident Analysis and Prevention*, vol. 124, no. September 2018, pp. 12–22, 2019.

[63] D. Gettman and S. Shelby, "Surrogate safety assessment model (SSAM)," Tech. Rep. 12, 2008.

[64] Z. H. Khattak, B. L. Smith, H. Park, and M. D. Fontaine, "Cooperative lane control application for fully connected and automated vehicles at multilane freeways," *Transportation Research Part C: Emerging Technologies*, vol. 111, no. November 2019, pp. 294–317, feb 2020.

[65] N. Virdi, H. Grzybowska, S. T. Waller, and V. Dixit, "A safety assessment of mixed fleets with Connected and Autonomous Vehicles using the Surrogate Safety Assessment Module," *Accident Analysis and Prevention*, vol. 131, no. December 2018, pp. 95–111, 2019.

[66] A. Sinha, S. Chand, K. P. Wijayaratna, N. Virdi, and V. Dixit, "Crash severity and rate evaluation of conventional vehicles in mixed fleets with connected and automated vehicles," *Procedia Computer Science*, vol. 170, pp. 688–695, 2020.

[67] C. Lu, X. He, H. van Lint, H. Tu, R. Happee, and M. Wang, "Performance evaluation of surrogate measures of safety with naturalistic driving data," *Accident Analysis and Prevention*, vol. 162, no. May, p. 106403, 2021.

[68] R. M. Brach, "Analysis of planar vehicle collisions using equations of impulse and momentum," *Accident Analysis & Prevention*, vol. 15, pp. 105–120, 4 1983.

[69] L. Cui, J. Hu, B. B. Park, and P. Bujanovic, "Development of a simulation platform for safety impact analysis considering vehicle dynamics, sensor errors, and communication latencies: Assessing cooperative adaptive cruise control under cyber attack," *Transportation Research Part C: Emerging Technologies*, vol. 97, no. June, pp. 1–22, 2018.

[70] R. Rajamani, *Vehicle Dynamics and Control*, ser. Mechanical Engineering Series. Boston, MA: Springer US, 2012.

[71] D. Bevly, X. Cao, M. Gordon, G. Ozbilgin, D. Kari, B. Nelson, J. Woodruff, M. Barth, C. Murray, A. Kurt, K. Redmill, and U. Ozguner, "Lane Change and Merge Maneuvers for Connected and Automated Vehicles: A Survey," *IEEE Transactions on Intelligent Vehicles*, vol. 1, no. 1, pp. 105–120, mar 2016.

[72] R. Attia, R. Orjuela, and M. Basset, "Combined longitudinal and lateral control for automated vehicle guidance," *Vehicle System Dynamics*, vol. 52, no. 2, pp. 261–279, feb 2014.

[73] P. Ioannou and C. Chien, "Autonomous intelligent cruise control," *IEEE Transactions on Vehicular Technology*, vol. 42, no. 4, pp. 657–672, 1993.

[74] R. Rajamani and C. Zhu, "Semi-autonomous adaptive cruise control systems," *IEEE Transactions on Vehicular Technology*, vol. 51, no. 5, pp. 1186–1192, sep 2002.

[75] PTV Group, "PTV VISSIM 10 User Manual," *PTV AG: Karlsruhe, Germany*, 2018.

[76] C. Xu, A. P. Tarko, W. Wang, and P. Liu, "Predicting crash likelihood and severity on freeways with real-time loop detector data," *Accident Analysis and Prevention*, vol. 57, pp. 30–39, 2013.

Data Management Plan

Products of Research
This study did not collect any data. All results are obtained from simulations in the commercial software VISSIM.

Data Format and Content
Not applicable.

Data Access and Sharing
Further details about the results obtained in this study can be obtained by contacting the authors at fvallada@usc.edu.

Reuse and Redistribution
The results from this work have no restrictions concerning reuse and redistribution by the general public.

Appendix: Collision Time Computation

In this appendix, we show how to compute the collision time under the worst-case braking scenario. From here on, we use the notation $g_0 = g(t_0)$ and $\Delta v_0 = v_\ell(t_0) - v_E(t_0)$, and we assume, without loss of generality, $t_0 = 0$. We find t_c by solving:

$$\begin{aligned} g(t_c) &= 0 \\ -\Delta g(t, t_c) &= g_0 \end{aligned}$$

where $\Delta g(t, t_c)$ is as defined in Eq.(1). The collision might occur during any of the 4 numbered time intervals shown in Figure 2. During each of them, the leading vehicle might be either at full stop or still decelerating by the time the collision occurs.

1. The collision occurs before the ego vehicle realizes the leader is braking, that is, $t_c < \tau_d$ if

$$g_0 < \tau_d \left[\frac{\bar{a}_E + d_\ell}{2}\tau_d - \Delta v_0\right]. \quad \textbf{(A. 1)}$$

The collision time and severity also depends on how fast the leading vehicle achieves full stop. If the leader is already traveling at slow speeds at t_0, it is possible that $t_\ell < \tau_d$. If

$$g_0 < t_\ell \left[\frac{\bar{a}_E + d_\ell}{2}t_\ell - \Delta v_0\right], \quad \textbf{(A. 2)}$$

the collision happens when the leader is still braking. Otherwise, the collision happens when the leader is at full stop. With this we can compute the collision time:

$$\mathrm{t_c} = \begin{cases} -\mathrm{v_E}(0) + \left(\mathrm{v_E^2}(0) + \bar{\mathrm{a}}_\mathrm{E}\left(2\,\mathrm{g_0} + \frac{\mathrm{v_\ell^2}(0)}{\mathrm{d_\ell}}\right)\right)^{\frac{1}{2}} \Big/ \bar{a}_E & \text{, if (A. 1) is true and (A.2) is false} \\ \Delta \mathrm{v_0} + \left(\Delta \mathrm{v_0^2} + 2\mathrm{g_0}\,(\bar{\mathrm{a}}_\mathrm{E} + \mathrm{d_\ell})\right)^{\frac{1}{2}} \Big/ \bar{a}_E + d_\ell & \text{, if (A.1), (A.3) are true} \end{cases}$$

We note that the first case above is only possible if $t_\ell < \tau_d$.

2. The collision occurs between τ_d and $\tau_d + \tau_j$ if inequality (A. 1) is false and

$$g_0 < (\tau_d + \tau_j)\left[\frac{\bar{a}_E + d_\ell}{2}(\tau_d + \tau_j) - \Delta v_0\right] - \frac{j_E}{6}\tau_j^3. \quad \textbf{(A. 3)}$$

Again, we have to consider the possibility of the leader achieving full stop before collision. If:

$$g_0 < t_\ell \left[\frac{\bar{a}_E + d_\ell}{2}t_\ell - \Delta v_0\right] - \frac{j_E}{6}\tau_j^3 \quad \textbf{(A. 4)}$$

the collision happens before the leader is at full stop. The collision time is:

$$t_c = \begin{cases} \text{root of (A.5), if (A.1) is false, (A.3) is true, and (A.4) is false} \\ \text{root of (A.6), if (A.1) is false and (A.3), (A.4) are true} \end{cases}$$

where the equations are:

$$\frac{j_E}{6}t_c^3 - \frac{1}{2}[\bar{a}_E + j_E\tau_d]t_c^2 + \left[\frac{j_E\tau_d^2}{2} - v_E(0)\right]t_c + g_0 - \frac{j_E\tau_d^3}{6} + \frac{v_\ell}{2d_\ell} = 0 \quad \textbf{(A. 5)}$$

$$\frac{j_E}{6}t_c^3 - \frac{1}{2}[\bar{a}_E + d_\ell + j_E\tau_d]t_c^2 + \left[\frac{j_E\tau_d^2}{2} + \Delta v_0\right]t_c + g_0 - \frac{j_E\tau_d^3}{6} = 0 \quad \textbf{(A. 6)}$$

3. The collision occurs after the ego vehicle achieves maximum deceleration but before it achieves full stop, i.e., $\tau_d + \tau_j \le t_c < t_E$ if:

$$g_0 < g^*(t_0). \quad \textbf{(A. 7)}$$

For the collision to occur in this interval with a leader that is still braking, it is necessary that:

$$g_0 < t_\ell\left[\frac{|d_\ell - d_E|}{2}t_\ell - \Delta v_0 + \lambda_1\right] + \lambda_0 \quad \textbf{(A. 8)}$$

Otherwise, the collision occurs when the leader is already at full stop. The collision time is:

$$t_c = \begin{cases} \Delta v_0 - \lambda_1 \pm \left((\lambda_1 - \Delta v_0)^2 + 2(g_0 - \lambda_0)(d_\ell - d_E)\right)^{\frac{1}{2}} \Big/ d_\ell - d_E, \\ \text{if (A.3) is false, (A.7) is true, and (A.8) is true} \\ \lambda_1 + v_E(0) - \left((v_E(0) + \lambda_1)^2 - 2(g_0 + v_\ell^2(0)/2d_\ell - \lambda_0)d_E\right)^{\frac{1}{2}} \Big/ d_E, \\ \text{if (A.3) is false and (A.7), (A.8) are true} \end{cases}$$

4. If inequality (A. 7)is false, there is no collision.